2014

Downstream spatial and temporal response to dam removal, White Salmon River, WA

Erika J. Colaiacomo
The University of Montana

DOWNSTREAM SPATIAL AND TEMPORAL RESPONSE TO DAM REMOVAL, WHITE SALMON RIVER, WA

By

Erika Jean Colaiacomo

B.A. Geology, Colgate University, Hamilton, NY, 2007

Thesis

presented in partial fulfillment of the requirements
for the degree of

Master of Science
in Geosciences

The University of Montana
Missoula, MT

Summer 2014

Approved by:

Sandy Ross, Dean of The Graduate School
Graduate School

Dr. Andrew Wilcox, Chair
Department of Geosciences

Dr. Johnnie Moore
Department of Geosciences

Dr. Lisa Eby
College of Forestry & Conservation

Colaiacomo, Erika J., M.S., Summer 2014 Geosciences

Downstream Spatial and Temporal Response to Dam Removal, White Salmon River, WA

Committee Chair: Dr. Andrew Wilcox

The Condit Dam breach on the White Salmon River (WSR) in Washington provided a unique opportunity to study how a bedrock-confined, gravel-bed river responds to a large influx of fine reservoir sediment. On October 26, 2011, a dynamite explosion breached a hole in the base of the 38 m tall dam, causing rapid reservoir erosion and downstream transport of fine sediment through the 5,300 m of channel separating the reservoir from the mouth of the WSR, where it flows into the Columbia River. In my research, I combined field data, aerial photographs, and LiDAR surveys to measure pre-breach and post-breach geomorphic conditions, up to 9 months after the breach, to assess downstream geomorphic response through a confined reach (reach 1) with forced pool-riffle morphology and a less-confined reach (reach 2) near the river's mouth. I found that the magnitude and duration of geomorphic adjustment was smaller over riffles than pools and over reach 1 than reach 2. By 3 weeks after the dam breach, pools stored about twice as much of the reservoir-derived sediment (~95,000 m^3) as riffles (~50,000 m^3). By 9 months post-breach, nearly all (90%) of the sediment had been evacuated from riffles (~5,000 m^3 remained), whereas about half of the sediment initially stored in pools had been evacuated (~50,000 m^3 remained). Reach 1 stored ~145,000 m^3 within the 3 weeks after the dam breach compared to the 650,000 m^3 stored in reach 2. By 9 months post-breach, the volume of sediment stored in reach 1 (~40,000 m^3) decreased by 72% and the volume in reach 2 (~490,000 m^3) decreased by only 25%. I also found significant storage behind large wood deposits and throughout the transition between reach 1 and reach 2. My findings suggest a conceptual model by which reductions in grain and bedform roughness caused by initial sediment deposition in reach 1 contribute to sediment transport and deposition in reach 2. Findings from the WSR can help inform recovery from other sediment disturbances and dam removals.

ACKNOWLEDGEMENTS

I would like to extend my sincere thanks to the following individuals, without whom this research would not have been possible. Firstly, I thank Dr. Andrew Wilcox for his invaluable comments and edits, patience, and financial assistance. I am grateful for the helpful comments and support provided by the UM Geomorphology lab group: Sharon Bywater-Reyes, April Sawyer, Kurt Imhoff, Franklin Dekker, Elena Evans, Andrea Stanley, Rebecca Manners, and Phairot Chatanantavet. I thank the following individuals for their field and logistical assistance: Rob Livesay, Sharon Bywater-Reyes, Elena Evans, Ben Gardner, Caitlin Alcott, Gardner Johnston, Josh Epstein, Jon Major, and Steve Stampfli. Thank you to Todd Olson and Tom Hickey from Pacificorp, Larry Moran from J.R. Merit, and Garth Wilson from Kleinfelder for providing site access and safety guidance. The survey data shared by the USGS Columbia River Research Laboratory and Kleinfelder greatly enhanced the scope of my analysis. Funding was provided by the National Science Foundation (EAR-0922296, EPS-1101342), Montana Water Center, and Geological Society of America. Lastly, I'm endlessly thankful for the unwavering support and encouragement from my family and friends.

Table of Contents

Figures

Tables

INTRODUCTION

Dam removals have increased in recent decades due to a combination of rising environmental and ecological awareness and aging dam infrastructure (American Rivers, 2012). Most of the 80,000 dams in the United States, the majority of which are less than 15 m tall, were built from 1950 through 1970 (Doyle et al., 2003). Most dam removals have been small (e.g. Sawaske & Freyberg, 2012), but recent removals of larger dams have exposed unprecedented amounts of reservoir sediment to erosion and downstream transport (Magirl et al., 2010). The potential geomorphic and ecological impacts of such events emphasize the need for detailed pre- and post-removal studies to better quantify and predict the magnitude and duration of post-removal channel response.

Dam removals can disturb a river system by releasing large amounts of accumulated reservoir sediments downstream and provide the opportunity to study river response to such disturbances. The erosion and transport of reservoir sediment following dam removals is analogous to natural sediment disturbances, such as landslides or volcanic eruptions (e.g. Gran and Montgomery, 2005), and assessments of downstream geomorphic response from disturbance provide a useful framework from which to assess dam removal (Doyle et al., 2002). Numerous factors control the fate of sediment pulses including downstream morphology, the nature of the dam breach, the volume and texture of reservoir sediment, and the annual hydrograph (e.g. Pizzuto, 2002).

The unique morphologies of mountain rivers influence the downstream response to dam removal in these settings. Mountain rivers have higher slopes, narrower valley bottoms, and more resistant channel boundaries than alluvial rivers (Rathburn & Wohl, 2003; E. Wohl, 2010). Mountain rivers can be bedrock-dominated or -influenced, with undulating canyon walls

that create lateral obstructions, flow convergence, pool scour, and forced pool-riffle morphologies (Thompson, 2010; Wohl et al., 1999). Instream wood can also influence local scour and deposition and morphology in mountain rivers (E. Wohl, 2011).

Within mountain rivers, reaches and bedforms may have different response potentials to sediment disturbance. The potential transport or storage of sediment in a reach depends upon the transport capacity of the reach and the sediment supply to the reach (Montgomery & Buffington, 1997). Transport capacity is a function of the boundary shear stress, which depends on flow depth and slope, and the critical shear stress for motion, which depends on bed-material properties, and can be quantified in terms of the bedload transport rate (Wilcock et al., 2009). Changes in any of the components of boundary shear stress or critical shear stress, such as changes in flow depth, slope, or grain size, will result in altered transport capacity and transport rates. Likewise, changes in sediment supply can influence both transport rates and sediment storage.

Studies of the geomorphic response to dam removals highlight how changes in confinement and bedform type influence transport capacity, sediment supply, and associated geomorphic response. For example, 1-D model predictions of channel response from the 2011-2014 removals of the Elwha and Glines Canyon dams from the Elwha River, Washington suggested that sediment would be deposited in areas of low transport capacity, such as upstream of valley constrictions, downstream of valley expansions, and in low-gradient reaches (Konrad, 2009), with potential negative effects on benthic invertebrates and salmon spawning gravels (Czuba et al., 2011; Konrad, 2009).

Downstream sediment storage near dam sites has been documented following dam removals. After the 2007 Brownsville Dam removal from the Calapooia River, Oregon, the

majority of sediment deposition occurred within the first 450 m downstream of the dam and caused channel narrowing and increases in bar area (Walter & Tullos, 2010). Pre-breach 1-D modeling of the 2009 removal of the Savage Rapids Dam from the Rogue River, Oregon predicted temporary deposition of reservoir sediment followed by scour in the 18 pools within the first 19 km downstream of the dam (Bountry, Lai, & Randle, 2013). However, surveys within the first year following removal documented complete infilling of a 5 m-deep scour pool immediately below the dam, partial infilling of the first natural, 5 m-deep pool downstream, but no further deposition in pools downstream (Bountry et al., 2013). Within one month after the 2007 breach of Marmot Dam on the Sandy River, Oregon, a wedge of bed aggradation up to 4 m thick stored 50% of the total eroded reservoir sediment within the first 1.3 km downstream of the dam (Major et al., 2012).

Following the removal of Marmot Dam, pools may have stored significant sediment volumes in otherwise high-transport reaches. From 2-9 km downstream from the dam, the Sandy River flows through a highly-confined gorge reach that pre-breach modeling suggested would transport sediment downstream, resulting in significant deposition below the gorge reach (Cui & Wilcox, 2008). However, post-breach surveys showed negligible deposition downstream of the gorge (Major et al., 2012). Up to 15% of sediment eroded from the reservoir was estimated to have been stored in pools within the first year, and sediment infilling of 2-3 m-deep pools was observed in the gorge 18 months after the breach (Major et al., 2012).

Downstream deposition in pools was also documented following a 1996 reservoir release on the North Fork Poudre River, Colorado. Wohl and Cenderelli (2000) measured preferential sediment deposition in pools and scour from upstream pools resulting in downstream pool deposition, followed by evacuation of between 80–90% of sediment infilling

pools by flows within one year. They emphasize the impact of downstream distance from the dam and the magnitude and duration of flows following the reservoir release in determining patterns of sediment deposition and transport (Wohl & Cenderelli, 2000). Rathburn and Wohl (2003) expand upon the post-release sediment dynamics on the North Fork Poudre and suggest a conceptual model in which channel gradient is the primary factor determining downstream transport and deposition, followed by channel complexity, such as pool and riffle bedforms.

Results from the 2007 Barlin Dam failure in Taiwan and the 2008 removal of the Milltown Dam from the Clark Fork River, Montana document the influence of channel confinement in promoting sediment transport. Tullos and Wang (2013) observed an average 2 m more deposition in a wider reach 1.3 km downstream of the dam than in the narrower reach immediately downstream of the dam. Valley width controlled sediment response near the dam, and they did not observe a correlation between decreasing geomorphic response with increasing downstream distance until ~3 km downstream of the dam (Tullos & Wang, 2014). Similarly, Evans and Wilcox (2014) report that the largest amount of downstream deposition on bars, the floodplain, and in side channels occurred 16 km downstream from the dam when the Clark Fork emerged from a high-transport, leveed reach flowing through the town of Missoula.

Using the geomorphic concepts of transport capacity and sediment supply illustrated by previous dam removals, I document and analyze the downstream geomorphic response of the White Salmon River (WSR), Washington to the breach and removal of Condit Dam. On October 26, 2011, a dynamite explosion breached a 5-m-wide hole in the base of the 38 m tall dam, causing rapid reservoir erosion and downstream transport of fine sediment through the 5.3 km separating the reservoir from the mouth of the WSR, where it flows into the Columbia River. I assess downstream geomorphic response through a confined reach (which I refer to as reach 1)

with forced pool-riffle morphology and a less-confined reach (which I refer to as reach 2) near the river's mouth. I predict that ratios of transport capacity and sediment supply, caused by changes in confinement and slope and mediated by discharge, will dictate channel response such that 1) at the bedform scale, riffles will exhibit a smaller magnitude and duration of geomorphic adjustment than pools, and 2) at the reach scale, the steep and confined reach 1 will exhibit a smaller magnitude and duration of geomorphic adjustment than reach 2.

I quantify the magnitude and duration of geomorphic adjustment with repeat measurements of water surface and bed elevations and grain size. I analyze ground photographs to determine the rate of initial bed aggradation and aerial photographs to document planform changes in reach 2. I calculate locations and volumes of geomorphic change from my repeated measurements of bed elevation, and I also calculate estimated bedload transport from my grain size and cross section surveys. I find support for my two predictions, and also observe variations in local sediment storage due to distance downstream from the dam, large wood dynamics, and the transition in transport capacity between reach 1 and reach 2. I also use findings from the WSR response to develop a conceptual model describing the downstream evolution of transport and storage after a sediment disturbance.

STUDY AREA

Located in south-central Washington, the 1,010 km^2 WSR watershed extends from the southwestern face of Mount Adams to the Columbia River (Figure 1). Basaltic bedrock underlays the watershed, and the WSR is bedrock-controlled with limited deposition of alluvial sediment along much of its course. The river has a mean annual discharge of 32 $m^3 s^{-1}$ and a mean annual peak discharge of 162 $m^3 s^{-1}$, largely due to rain and rain-on-snow events occurring between November and March. Discharge has been measured at the USGS White Salmon River near Underwood, WA USGS gage (#14123500), 2,350 m downstream of the Condit Dam site, since 1912.

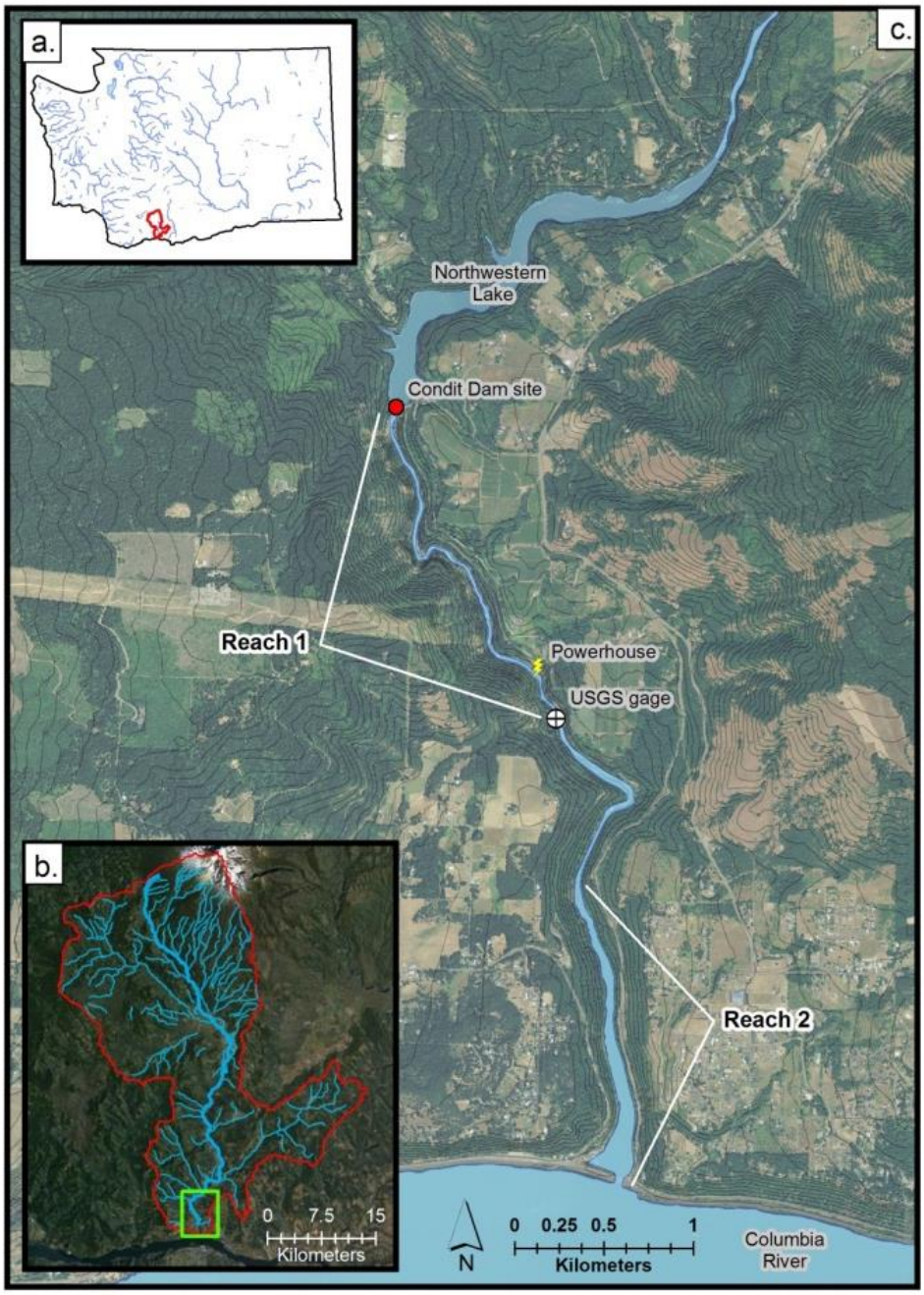

Figure 1: Field map. a. Location of the White Salmon watershed in southern Washington; b. Aerial map of the watershed, which extends southward from Mount Adams to the Columbia River; study reach is outlined in green; c. Aerial photo of the study reach, showing the locations of the dam, powerhouse, gage, and reach 1 and 2.

Condit Dam was built in 1913 to provide power to the growing regional logging industry and had a maximum 15 MW generating capacity (PacifiCorp Energy, 2002). The dam was located 5,300 m upstream from the river mouth, and a wooden stave pipeline approximately 4 m in diameter diverted flow 2,100 m downstream from the dam site to the powerhouse, creating a bypass reach (PacifiCorp Energy, 2002) (Figures 1 and 2). Minimum flows in the bypass reach averaged 5.7 $m^3 s^{-1}$ throughout the most of the year and decreased to 4.3 $m^3 s^{-1}$ from July 1 to August 15 (CH2M HILL, 2002). The 38 m-tall Condit Dam impounded Northwestern Lake, which extended 2,900 m upstream and had a surface area of 37 hectares. Reservoir sediment totaled 1.76 million m^3 and consisted of 60% sand, 30% silt, 7% clay, and 3% gravel (PacifiCorp Energy, 2006) .

The decision to remove Condit Dam came as the result of Pacificorp, the dam owner, applying to the Federal Energy Regulatory Commission (FERC) for relicensing in 1991 (WA Dept of Ecology, 2007). In 1996, FERC released the Final Environmental Impact Statement for the dam, specifying fish passage as a mandatory requirement for relicensing (WA Dept of Ecology, 2007). Pacificorp decided that retrofitting fish passage to the dam would be cost-prohibitive and opted for removal (WA Dept of Ecology, 2007). Removal of the dam provided anadromous salmonid access to up to 51.5 river kilometers of habitat (WA Dept of Ecology, 2007).

On October 26, 2011, contractors used explosives to breach a 5-m-wide tunnel drilled into the dam at its base, releasing a peak flow of 421 $m^3 s^{-1}$, and causing a rapid drop in reservoir base level and subsequent liquefaction, massive land sliding, and erosion and transport of reservoir sediment downstream (Figure 2) (Wilcox et al., 2014). Over the following year, contractors removed the dam, with most of the removal activity occurring after spring 2012 high flows (Figure 2c). Grading of the banks of the former reservoir began several weeks after the breach. The breach exposed a ~2.5 m-tall cofferdam used during the original dam construction

(PacifiCorp Energy, 2012). Contractors removed the cofferdam in April of 2012, thus removing the last barrier to upstream fish migration. The dam was completely removed by September 2012.

Figure 2: Time-lapse photography taken on river right hillslope about 100 m downstream from dam site: a. A typical pre-breach condition; b. explosive dam breach, ~50 seconds after the explosives detonation that breached the dam; c. progressive removal of dam structure, 8.5 months after the breach; d. dam site after the removal, 10.5 months after the breach (photos courtesy of S. Stampfli and A. Maser).

I define two geomorphic reaches between the dam site and the mouth of the WSR: 1) reach 1, a steep, confined reach extending from the dam site to 2,300 m downstream, and 2) reach 2, a low-gradient, less-confined reach from 3,600 m downstream of the dam to the river's mouth and confluence with the Columbia River. Average valley width in reach 1 is 20 m and average bed slope is 0.008. Narrow, undulating canyon walls create lateral obstructions, forming forced pool-riffle morphologies throughout the reach. Prior to the dam breach, the bypass reach, created by flow diversion through the pipeline from the dam to the powerhouse,

encompassed the majority of reach 1, creating quiet, low-velocity pools and shallow riffles with exposed boulders and bedrock. Average valley width in reach 2 is 80 m, which is 4 times wider than reach 1 and bed slope is 0.004, or half the slope of reach 1. Bonneville Dam, 30 km downstream from the mouth of the WSR on the Columbia River, causes a backwater effect on the Columbia River that extends approximately 1,000 m upstream into reach 2. Bonneville Dam operations cause the water level of the Columbia River to fluctuate by a maximum of 1.5 m throughout the year. The lower portion of reach 2 is referred to locally as the "In-Lieu Site," after a site near the mouth providing tribal fishing access.

METHODS

I combined my field data with data collected by agencies and contractors. I completed three sets of field surveys: ~2 months before the breach (summer 2011), ~3 months post-breach (January 2012), and 9 months after the dam breach (summer 2012) (Table 1). Data from agencies and contractors included aerial photography, LiDAR, time-lapse images, and echosounder bathymetry (Table 1).

Field and remote sensing observations of geomorphic responses were interpreted in the context of post-breach flows. The dam breach returned full flows to the bypass reach that encompassed the majority of reach 1. Natural and seasonal flows, as measured at the USGS White Salmon River near Underwood gage (Figure 3), influenced post-breach responses. A 37 $m^3 s^{-1}$ flow event occurred between the dam breach and the 2 months post-breach LiDAR flight, and another 50 $m^3 s^{-1}$ event occurred between the LiDAR flight and 3 months post-breach field survey (Figure 3). Flows increased after the 3 months post-breach field survey, reaching a peak of 156 $m^3 s^{-1}$ at the end of March. By the 9 months post-breach field survey, flows had returned to baseflow levels.

Table 1: Dates, timing relative to breach, and discharge associated with each survey type.

Survey type	Date(s)	Timing relative to breach	Discharge (cms)
Field	Aug 3-22, 2011	pre-breach	23.2 - 32.6
Aerial Photography	Nov 2, 2011	1 week post-breach	22.7
LiDAR	Dec 21, 2011	2 months post-breach	21.5
Field	Jan 6-18, 2012	3 months post-breach	24.1 - 31.1
LiDAR	Jul 28, 2012	8 months post-breach	26.7
Aerial Photography	Aug 6, 2012	9 months post-breach	24.2
Field	Jul 24 - Aug 16, 2012	9 months post-breach	21.0 - 27.9

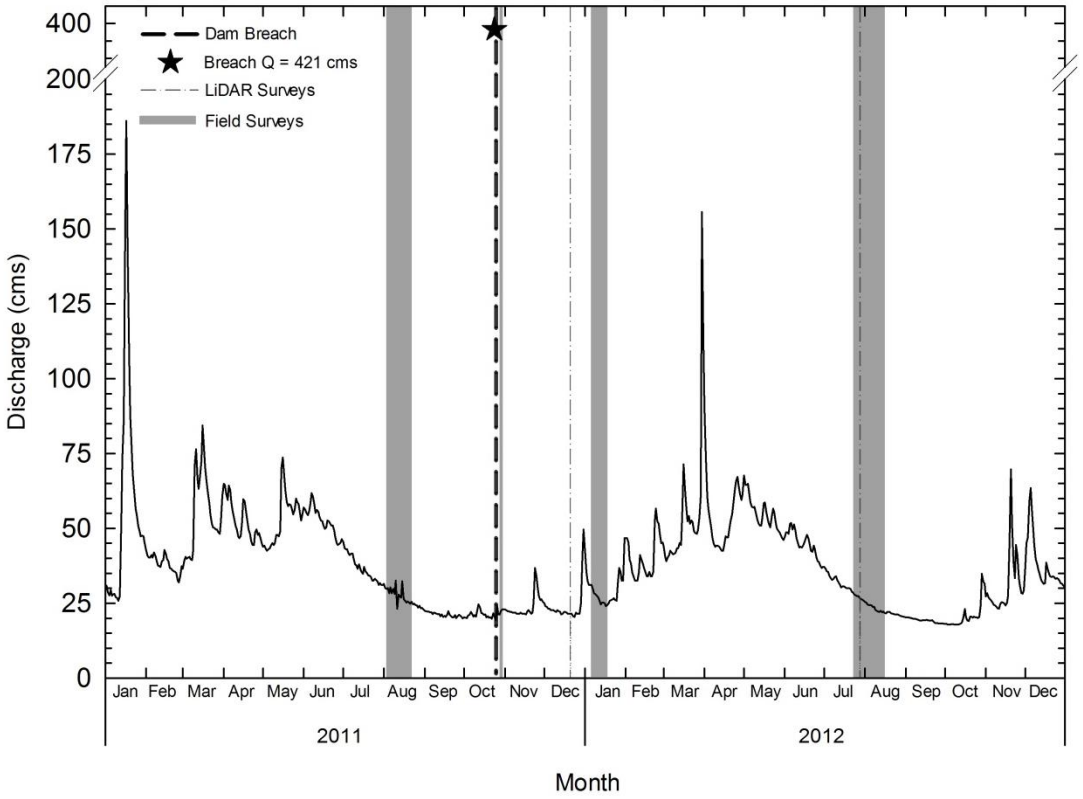

Figure 3. Average daily flows from January 1, 2011 to December 31, 2012 from the White Salmon River near Underwood, WA USGS gage 14123500. Light grey vertical bars represent field survey durations (see table 1), and 2 dotted grey vertical lines are the dates of two LiDAR surveys.

Surveys of topographic and textural changes

To assess pre-breach topographic and transport conditions in reach 1, I measured bed elevations of pools and riffles and grain size of riffles. To measure pre-breach riffle topography, I surveyed 12 cross sections on riffles in summer 2011 using a Leica FlexLine TS06 total station. I also measured grain size at these locations using Wolman pebble counts (Wolman, 1954). To measure pre-breach pool topography, in 10 pools I surveyed an approximate grid of points from a kickboat, where the water surface position was surveyed with the total station and the corresponding depth was measured using a weighted tape. To develop digital elevation models (DEMs) over pools, I first subtracted my measured depths from the average pool water surface

elevation to calculate the bed elevation at each point. Then I used the bed elevations to create 2.5-m-resolution DEMs in ArcGIS.

Post-breach surveys of riffles and pools in reach 1 were largely unsuccessful as a result of increased flows, compared to pre-breach conditions, in the bypass reach. Therefore, I used several alternative methods to infer post-breach geomorphic changes. Three months after the breach, I surveyed the surface of a newly-deposited, laterally discontinuous sand deposit along the river canyon walls as well as the elevation of a muddy deposit that had coated the canyon walls. During my 9 months post-breach field survey I accessed and resurveyed 4 out of my 12 original pebble counts. I also collected 10 bulk samples (~1 kg/sample) from the sand deposit at approximate riffle cross section locations.

As an alternative to directly measuring post-breach bed topography in reach 1, I back-calculated bedform depths over pools and riffles using measurements of discharge (from the USGS gage), float velocities, and width during my 9 months post-breach field survey. I measured wetted width 3-4 times along the length of each bedform (i.e., pool or riffle) with a Leica Disto D8 Laser Distance Meter. I measured velocities based on travel time of wood tossed into the channel, from the upstream to the downstream end of the bedform of interest. I completed 5 to 6 repetitions per bedform, in an attempt to measure velocities across the width of the channel. I divided bedform length by the average float time to calculate an average velocity, and I multiplied the resulting surface velocity by 0.86 to calculate a depth-averaged velocity (Mosley & McKerchar, 1993). I divided the average daily discharge by the depth-averaged velocity to calculate a feature cross-sectional area, and extracted feature depth by solving the area of a semi-ellipse for height, using the average bedform width and area. Finally, to determine post-

breach bed elevations of these bedforms, I subtracted depth from the average water surface elevation for each feature.

To assess topographic changes in reach 2, I primarily used pre-breach and summer 2012 multi-beam echosounder bathymetric measurements and robotic RTK topography collected by the US Geological Survey (U.S. Geological Survey, 2012)(Table 1). I supplemented these with my own field survey data. Three months post-breach, I surveyed 7 cross sections in reach 2 on two newly-deposited alternating bars near the river mouth. I surveyed the channel bed by floating downstream past the two bars 14 times with a SonarMite single-beam echosounder and Trimble GeoXH 6000 GPS, and I attempted to space the float paths evenly across the channel. I created a 1-m DEM of 3 months post-breach bed elevations in reach 2 by combining the elevation data points from my echosounder floats in the channel and cross sections on bars. I created 1-m DEMs of pre-breach and 9 months post-breach bed elevations in reach 2 in ArcGIS from the datasets provided by USGS.

I used time-lapse photography and USGS gage data to assess the rates and locations of bed elevation change at three additional locations. To document post-breach response at the dam site, I installed a time-lapse field camera on river left, 50 m downstream of the dam that took photos every 4 hours after the breach. To assess aggradation at the downstream end of reach 1, I evaluated changes in stage height at the USGS gage. I also used time-lapse photography from the river mouth (courtesy of D. Gathard). I visually examined the time-lapse photographs taken of the dam site and from the mouth to evaluate channel aggradation rates within the first 3 weeks following the breach. I defined maximum bed aggradation as the time that the sandy, lateral deposit first becomes continuously visible and bed elevations continue to decline.

Longitudinal profiles of bed and water-surface elevation

I combined the various data sources and methods described above to develop insight into post-removal geomorphic responses using several approaches. One of these was to develop pre- and post-breach longitudinal profiles of bed and water surface elevations from the dam site to the mouth. To calculate pre- and post-breach bed and water surface elevations (WSEs), I first processed raw elevation data into DEMs.

I developed bed elevation profiles in reach 1 from my pre-breach and 9 month post-breach field measurements. For the pre-breach bed-elevation profile in reach 1, I extracted thalweg elevations both from my cross section surveys over riffles and from cross sections extracted from DEMs of pools (described above). For the 9-month post-breach bed elevation profile in reach 1, I used bed elevations over pools and riffles from my float velocity measurements (described above). I also created a longitudinal profile of the sand deposit, which is representative of bed elevation conditions at the time of maximum aggradation, by spatially joining the nearest sand deposit elevation points to points created along the thalweg (described below).

I also developed water surface elevation profiles, which allowed for more spatially-continuous data than the bed elevation profiles. Using pre-breach aerial photography as a guide, I hand-digitized the thalweg from the dam site to mouth and created points every 10 m along the thalweg. I then extracted water surface elevations for these points from field surveys of water surface and from DEMs. I created the pre-breach WSE profile by spatially joining the nearest surveyed water surface elevation points to points created along the thalweg. WSE profiles for 2 and 9 months post-breach were extracted from 1-m DEMs generated from LiDAR flights flown on December 21, 2011 and July 28, 2012 (Watershed Sciences Inc., 2012).

To calculate longitudinal variations in valley width, I manipulated the DEM from the July 28, 2012 LiDAR flight in ArcGIS. I calculated a slope raster from the DEM, and I created cross sections perpendicular to the thalweg at each point I used to extract WSEs. The cross sections extended from the river surface and up the valley walls. I created points every meter along each cross section, extracted the slope raster values to these points, and deleted any slope points that were greater than 4 degrees. I converted the points back to lines and calculated the length of each line to derive a valley width profile.

Planform and sediment storage changes

I analyzed aerial photography to assess planform change (Figure 3, Table 1). I manually digitized channel and bar polygons from pre-breach, 1 week post-breach, and 2 and 9 months post-breach aerial photography in ArcGIS. I supplemented these with data from 3 months post-breach field surveys. I also calculated bar and channel polygon areas from the digitized planforms in ArcGIS.

To further characterize topographic changes, I calculated downstream fluctuations in sediment storage from pre-breach conditions to 5 post-breach conditions: 24 hours post-breach, 1 week post-breach, the time of maximum aggradation of the sand bed, 8 weeks post-breach, and 9 months post-breach. I place my calculations in the context of reservoir erosion and deposition in the Columbia River, as documented by PacifiCorp Energy (2011) and Wilcox et al., (2014). In reach 1, I calculated sediment storage over 10 pools and 10 riffles. I calculated bed elevation change by subtracting pre-breach cross-section average bed elevations from the average sand bed elevation of a feature and by subtracting 9 month post-breach average bed elevations from sand bed elevations. I interpolated sand bed elevations over features that were not surveyed by averaging adjacent bed elevation measurements, taking the length of the

feature and distance between measurements into account. To interpolate post-breach bedform elevations over features that were not measured, I averaged post-breach riffle depths and pool depths, and subtracted the average riffle depth from the average riffle WSEs and the average pool depth from average pool WSEs. I multiplied calculated bed elevation changes by the average feature width and length to calculate the volume of sediment stored. I calculated errors in reach 1 by propagating error resulting from averaging the depths at each cross section.

To analyze changes in bed elevation and sediment storage in reach 2, I used Geomorphic Change Detection (GCD) software (ESSA Technologies, North Arrow Research, & Wheaton, 2012). The GCD software detects cell-by-cell changes in elevation between two survey DEMs to compute a DEM of difference (DoD), where cell values in the DoD represent the change in elevation from the earlier survey DEM to the later survey DEM. I computed changes between (a) my pre-breach DEM and the sand bed surface, (b) my pre-breach and 3 month post-breach DEMs, (c) my 3 and 9 month post-breach DEMs, and (d) my pre-breach and 9 month post-breach DEMs. To address potential errors in survey layers, I excluded any changes less than 0.1 m. In addition to creating the DoD, the GCD software uses cell resolution and elevation change to compute the volumes of erosion and deposition between two survey times, which I used to assess temporal changes in sediment storage

Changes in transport capacity

I used the Bedload Assessment for Gravel-bed Streams (BAGS) Microsoft Excel macro to calculate pre- and 9 month post-breach transport capacities on accessible riffles (Pitlick et al., 2009). BAGS includes several transport equations, and I chose the Wilcock and Crowe (2003) equation because it is a surface-based transport equation and accommodates the full grain size distribution of bed, thereby accounting for the non-linear influence of sand on gravel transport

rates (Pitlick et al., 2009). The equation requires inputs of channel cross section topography, reach-average water surface slope, bed surface grain size distribution, bed roughness, and a single discharge, or range of discharges, over which to calculate transport. For topography, I used my pre-breach cross section surveys to calculate pre-breach transport; however, because I was unable to resurvey cross-sections during post-breach conditions, I used the surveyed wetted width to calculate 9 months post-breach transport. I calculated water surface slopes from my WSE profiles and grain size distributions from my pebble counts, and I visually estimated Manning's roughness values (Barnes, 1967). I modeled transport during the Q_2 discharge, which I calculated as 130 $m^3 s^{-1}$ from gage data, for pre- and 9 months post-breach conditions.

RESULTS

Pre-breach morphology

Prior to the dam breach, the average bed slope in reach 1 was 0.0077 m m^{-1} versus 0.0039 m m^{-1} in reach 2, and average valley width was 18 m in reach 1 compared to 82 m in reach 2 (Figure 4). The rapid increase in floodplain width at ~3,600 m downstream indicates the beginning of reach 2 and fluctuations in floodplain width within reach 1 represent the undulation of canyon walls (Figure 4). Within reach 1, the average bed slope over riffles was 0.012 m m^{-1} versus 0.0084 m m^{-1} over pools (Figure 4). Pools depths averaged 2 m compared to the average 0.4 m depth over riffles.

Initial geomorphic response: Post-breach water and sediment pulse

The maximum water surface elevation reached by the breach discharge (peak = 421 m^3 s^{-1}) varied with pre-breach channel morphology and distance from the dam. Within the first 2 hours post-breach, flow receded to ~ 25 m^3 s^{-1} and revealed a continuous high-water mark along the canyon walls (Figure 5). The longitudinal profile of this mark shows that the maximum breach elevation within the first 100 m downstream of the dam site was 8.1- 8.8 m above pre-breach WSEs (Figure 4). The magnitude of difference between the pre-breach WSE and the high-water, post-breach peak WSE decreased in a downstream direction through reach 1 (Figure 4). At 3,200 m downstream, pre-breach WSE rapidly dropped as the river transitions from reach 1 to reach 2, whereas the high-water, post-breach peak WSE remained smoother through this reach, tapering toward the pre-breach WSE at the mouth (Figure 4). In reach 2, the difference between the pre-breach WSE and the post-breach peak WSE is partly attributable to Bonneville pool fluctuations (Appendix F).

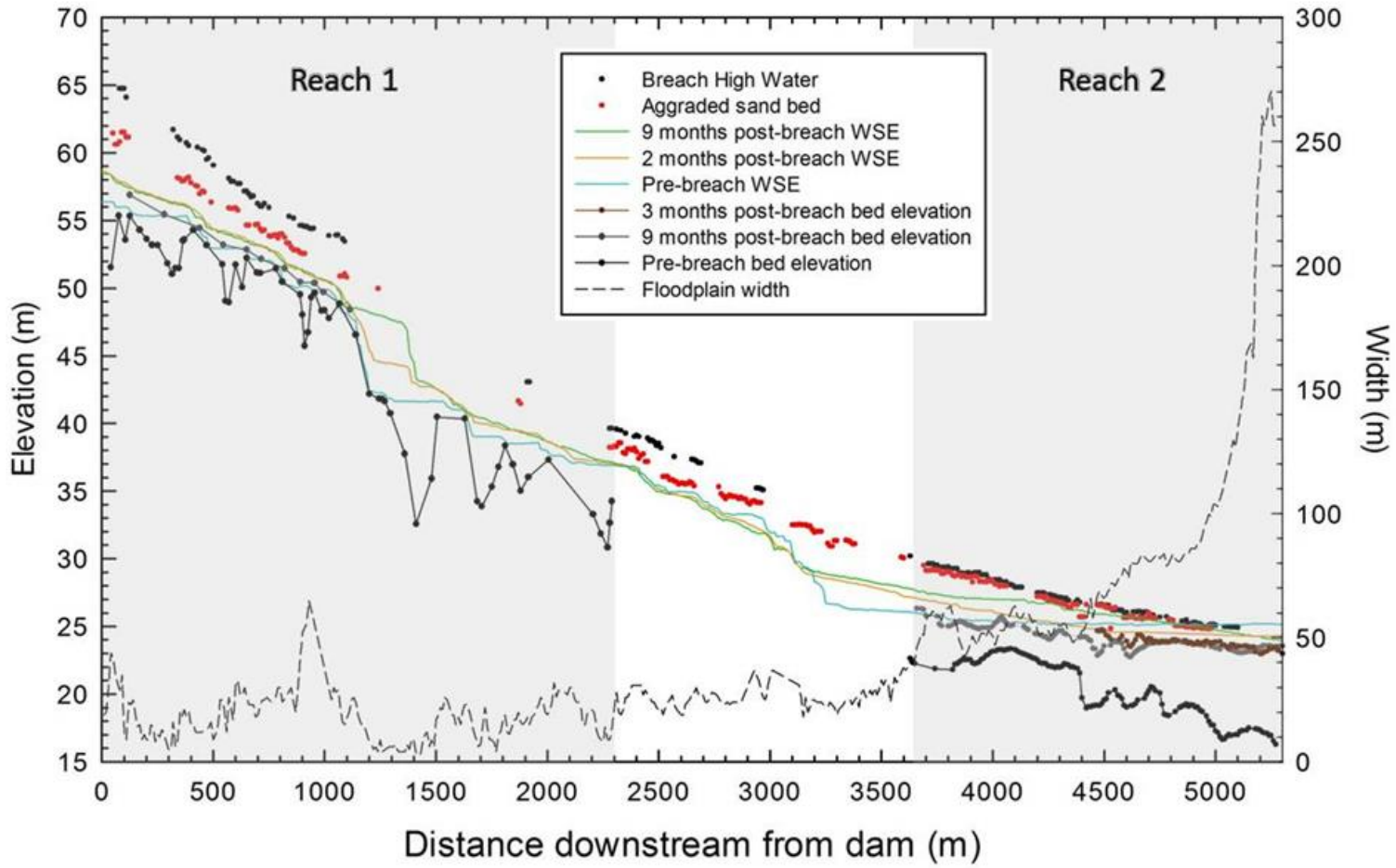

Figure 4: Longitudinal profiles of bed and water surface elevations (left Y axis) and valley width (right Y axis) versus distance downstream. Bed elevations are shown for pre-breach and 9 months post-breach for reach 1 and 2, as well as for 3 months post-breach in reach 2. The sand bed elevation reached within the first 3 weeks after the breach is shown throughout in the whole river as are pre-breach, maximum breach level, and 2 and 9 months post-breach water surface elevations.

Figure 5: Breach high water mark and lateral sand deposits (aggraded sand bed) at 600 m downstream of dam, river left, looking upstream (January 8, 2012 photograph, ~2.5 months after the breach). The maximum breach flow covered the lower portion of canyon walls downstream of the dam with a silty film and the sand bed deposited within the 3 weeks after the breach left a terrace along the banks after subsequent bed incision

Within the first 3 weeks following the breach, while discharge remained at ~ 22 $m^3 s^{-1}$, a sandy sediment pulse moved downstream from the dam to the mouth and caused the greatest amounts of bed aggradation observed during the 9 months after the breach. Field observations within the week following the breach and subsequent analysis of lateral deposits indicate that sand bedload transport and antidune migration occurred during bed aggradation. I observed antidune migration from the dam site to 1,000 m downstream over five days following the breach, and photographs of lateral sand deposits reveal low-angle cross-bedding (Appendix G).

At the dam, time-lapse photography indicates maximum bed aggradation occurred on October 29, 2011, three days after the breach, as inferred from changes in water levels against the face of the dam during times of steady discharge (Figure 6b). At the USGS gage 2,350 m downstream, analysis of stage indicates that the bed reached its maximum level of aggradation of 1.1 m above pre-breach conditions on November 7, 2011, 12 days post-breach (Figure 7). Photo analysis near the river mouth, 5,200 m downstream, reveals that the maximum sand bed aggradation occurred on November 13, 2011, 6 days after the maximum aggradation at the gage and 18 days after the breach. Dividing the downstream channel distance traveled by time yields a downstream travel rate for the zone of maximum aggradation of 196 m day^{-1} between the dam site and gage, 475 m day^{-1} between the gage and 5,200 m downstream of the dam (Figure 8b), and 289 m day^{-1} from the dam to the mouth.

Figure 6: Photographs illustrating changes in morphology and water surface elevations, indicative of post-breach sediment deposition, at Condit Dam site from river right. a) pre-breach conditions at the dam site, b) conditions at the time of maximum bed aggradation, and c) conditions after bed had incised from its maximum aggraded level.

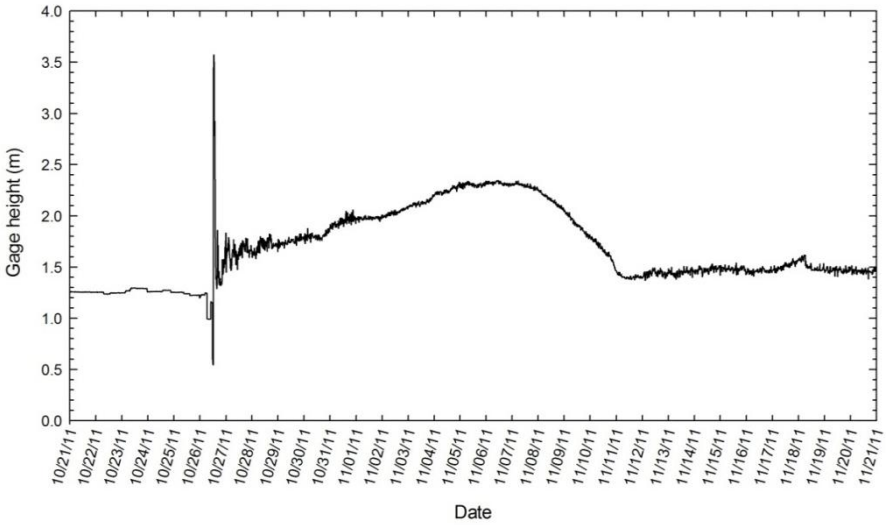

Figure 7: Hourly gage height from USGS gage (14123500) at 2,350 m downstream of dam site, from October 21 to November 21, 2011. Dam breach on October 26 shown as abrupt spike in height and maximum bed aggradation was reached on November 7, 2011.

Figure 8: Photographs illustrating changes in morphology and water surface elevations, indicative of post-breach sediment deposition, in reach 2, 5,200 m downstream from dam. a) pre-breach conditions at the mouth, b) conditions at the time of maximum bed aggradation, and c) conditions after bed had incised from maximum aggraded level.

The spatial pattern of the aggraded sand bed differs between reach 1 and reach 2. Comparison of the longitudinal profile of the aggraded sand bed to pre-breach elevations within the first 1,200 m downstream of the dam reveals that the magnitude of bed aggradation decreased with increasing distance downstream in reach 1. In reach 2, the sand bed elevation is approximately constant, and the difference between the elevation of the sand bed and pre-breach bed elevations increases with increasing distance downstream (Figure 4).

Geomorphic response from 2 to 9 months post-breach: Changes in water and bed surface elevations

Continuous profiles of WSE extracted from LiDAR surveys for both 2 and 9 months post-breach show an increase in WSE compared to pre-breach elevations (Figure 4). In reach 1, some of this increase is attributable to the return of full flows to the bypass reach. However, in general, changes in water-surface elevations are indicative of changes in bed elevations, and evolution of channel morphology during the winter and spring following the dam breach can be inferred from comparison of WSE profiles from 2 and 9 months post-breach.

A comparison of post-breach water surface profiles suggests that little net topographic change occurred in reach 1 between 2 and 9 months post-breach, but that topography continued to evolve in reach 2. The 2 and 9 months post-breach water surface profiles are similar to each other from the dam site to 1,200 m downstream (Figure 4). From 1,200 to 1,400 m downstream of the dam, the 2 and 9 month profiles differ in elevation by up to 3.5 m, due to the development of a log jam in this highly confined reach (Figures 4 and 9). From 1,400 to 3,100 m downstream, the profiles have similar elevations, although the 2 months post-breach profile has greater drops in elevation over riffles crests than the 9 months post-breach profile. From 2,450 to 3,150 m, both post-breach profiles are less than the pre-breach profile. At 3,350 m downstream, the 2 months post-breach profile is 1.95 m greater than the pre-breach profile and this elevation difference tapers until 4,300 m downstream, where the 2 months post-breach WSE is less than pre-breach values. Nine months post-breach WSEs remain over 2 m greater than pre-breach values from 3,250 to 3,500 m downstream, and then taper to pre-breach values by 4,880 m downstream.

When compared to the pre-breach water surface profile, both post-breach profiles show decreased slopes over riffles, increased slopes over pools, and an overall decrease in abrupt elevation changes. Furthermore, water surface slopes continued to evolve from 2 to 9 months over pools and reach 2, while slopes remained approximately constant over riffles and reach 1 on average. Average water surface slopes over riffles decreased from 0.016 to 0.012 m m^{-1} from pre-breach to 2 months post breach and remained at 0.012 m m^{-1} at 9 months post-breach. Over pools, average water surface slopes increased from 0.003 pre-breach to 0.005 m m^{-1} 2 months post-breach, and continued to increase to 0.008 m m^{-1} at 9 months post-breach. In reach 1, water surface slopes remained at 0.01 m m^{-1} on average from pre-breach to 2 and 9 months post-breach; however, in reach 2, average water surface slopes increased from 0.00099 pre-breach to 0.0012 m m^{-1} 2 months post-breach, and continued to increase to 0.0027 m m^{-1} by 9 months post-breach.

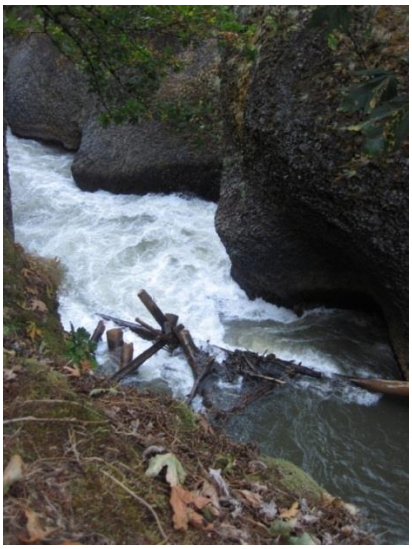

Figure 9: Log jam 1,400 m downstream of dam site (Aug 17, 2012 photograph).

After the initial period of bed aggradation, bed elevations decreased but remained greater than pre-breach conditions, particularly over pools and reach 2. From 125 to 1,100 m

downstream in reach 1, 9 month post-breach bed elevations are within 1 m of pre-breach bed elevations, but remain elevated over pools. Three months post-breach, bed elevations in reach 2 from 4,500 m downstream to the mouth remain elevated and are closer to the sand bed elevation than the pre-breach bed. Bed elevations 9 months post-breach in reach 2 remain approximately the same as bed elevations from 3 months post-breach from 4,750 m downstream to the mouth, and, 9 months post-breach bed elevations are an average 1.5 m less than 3 months post-breach elevations from 4,500 m to 4,750 m downstream.

Post-breach aggradation of the sand bed produced greater increases in bed elevation over pools than riffles, and 9 months post-breach bed elevations remained elevated in pools (Figure 4 and 9). Within the first 1,200 m downstream of the dam, the elevation change over pools was 5.2 ± 1.2 m versus the 3.3 ± 0.8 m over riffles. The largest bed elevation increase (8.0 m) was at the former plunge pool immediately downstream of the dam and the magnitude of elevation change over both pools and riffles decreased with increasing distance from the dam (Figure 10). Nine months post-breach, the channel in reach 1 had incised into the sandy bed deposit back toward the pre-breach bed elevation. The magnitude of this incision also decreased with distance from the dam; however, contrary to the aggradation of the sandy bed, the magnitude of bed elevation change did not differ over pools and riffles. Pool bed elevations decreased by 2.6 ± 0.5 m from the sandy bed elevation and riffles decreased by 2.6 ± 0.8 m. Overall the magnitudes of positive elevation changes are greater than negative changes, indicating net deposition.

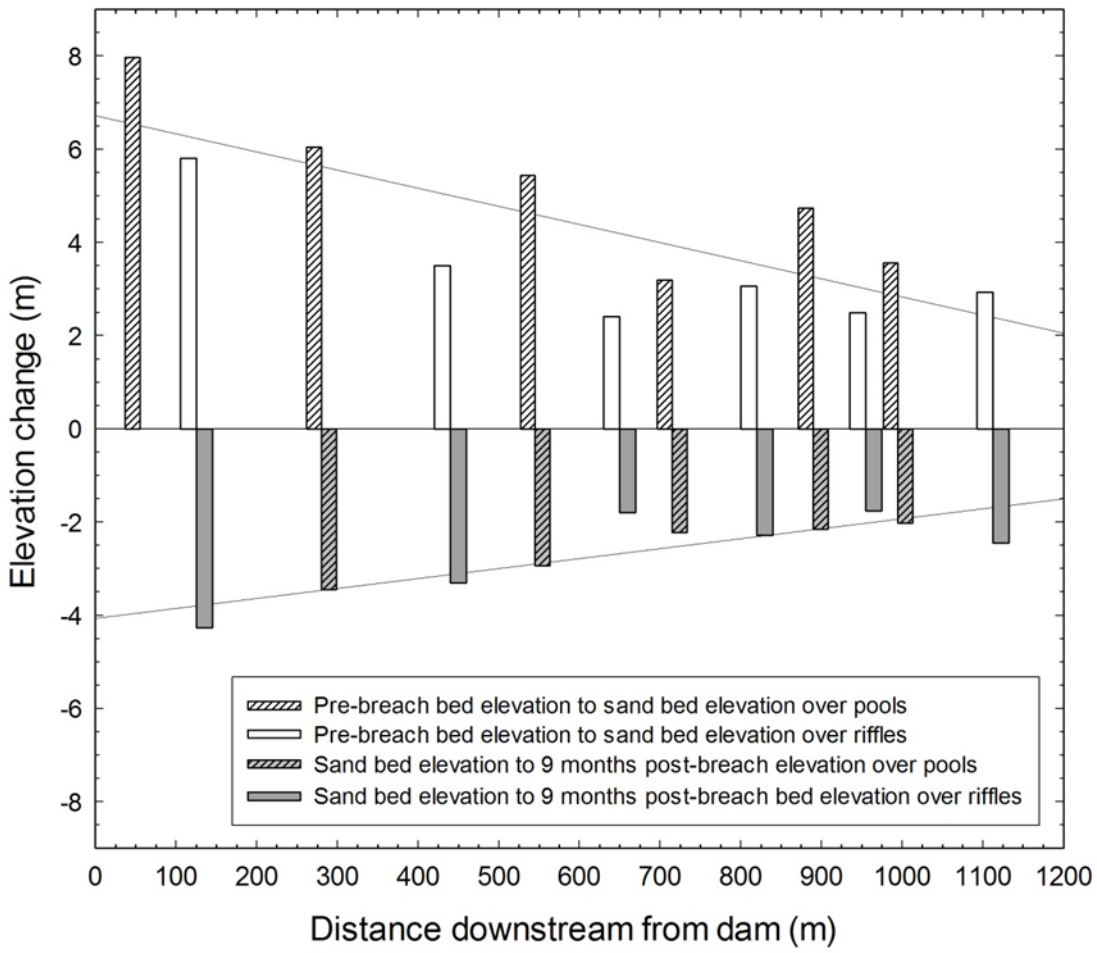

Figure 10: Changes in bed elevation from pre-breach to sand bed conditions and from sand bed to 9 months post-breach conditions for pools and riffles from the dam site to 1,200 m downstream. Positive elevation change denotes bed aggradation and negative elevation change denotes bed incision. Initial bed aggradation is less over riffles than pools and there is no significant difference in bed incision levels between pools and riffles. Both bed aggradation and incision decrease in magnitude with increasing distance from the dam as shown by regression trendlines. Nine months post-breach conditions show net positive bed elevation change over both pools and riffles, with greater elevation change over pools.

Persistent and large-magnitude aggradation occurred in reach 2. Pre-breach bathymetry influenced patterns of bed aggradation and incision (Figures 11 and 12). The aggraded sand bed likely draped the pre-breach bed in a planar fashion in reach 2. As a result, the smallest magnitude of deposition occurred in previously shallow areas along the channel margins, where pre-breach bathymetry showed alternate bar topography (Figure 11a); the average bed elevation change in these areas was ~3 m (Figure 12a). The largest magnitude of elevation change during this period was >9.5 m, just upstream from the mouth on river left where pre-breach bed elevation was lowest (Figure 12a). Farther upstream in reach 2, where the channel transitions away from the influence of the Bonneville pool's backwater and pre-breach depths were lower, the post-breach aggradation was between 4.5 – 5 m (Figures 11 and 12).

The majority of aggradation in reach 2 occurred as a result of sand deposition in the days and weeks after the breach, and subsequent incision and reworking occurred over 3 and 9 months post-breach. From the aggraded sand bed condition to 3 months post-breach, bed elevation decreased by about 1 m over bars and > 2.5 m in the newly-formed channel (Figure 12b). From 3 to 9 months post-breach, around 0.5 m of sediment was deposited on the alternating channel bars, and ~1.5 m of incision continued in the channel. The 9 months post-breach DEM shows reworking of the 2 lateral bars near the mouth by temporary side channels and localized incision and deposition (Figure 11). As of 9 months post-breach, bed elevation increases of up to 3 m from 3,600 to 4,400 m downstream of the dam and up to 6 m from 4,400 m downstream to the mouth, persisted in reach 2 compared to pre-breach bed elevations.

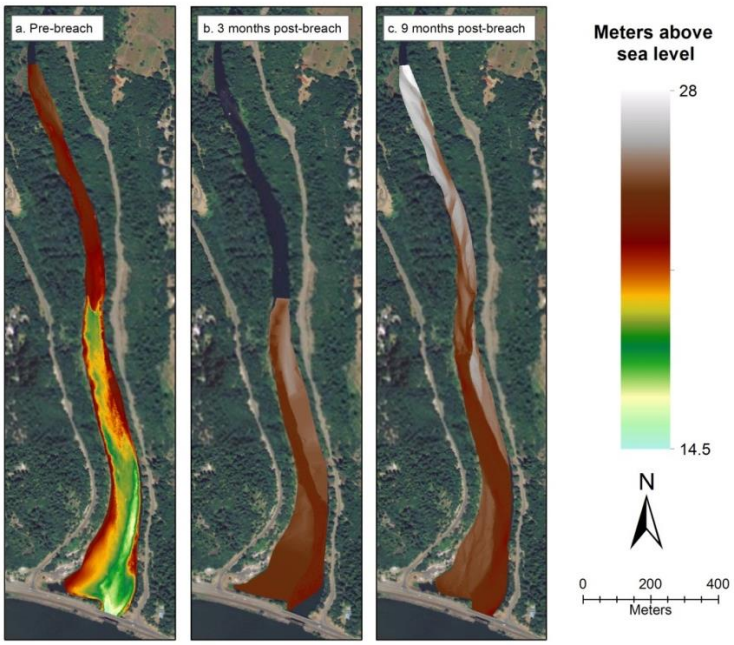

Figure 11: One-meter DEMs used in GCD in Figure 12. DEMs for a. pre-breach, b. 3 months post-breach, and c. 9 months post-breach shown.

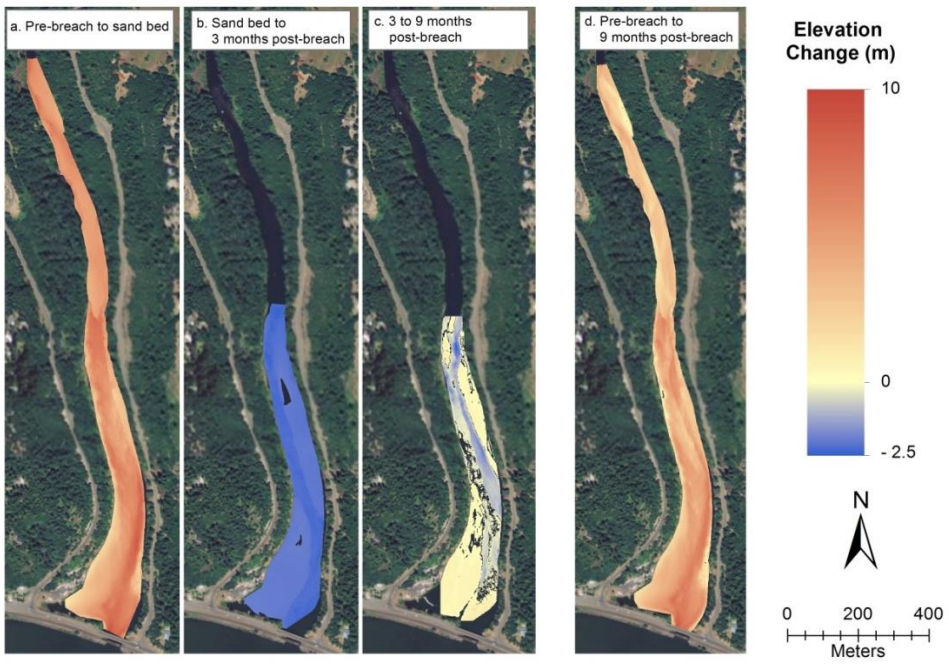

Figure 12: Geomorphic change detection (GCD) results comparing a. pre-breach to sand bed, b. sand bed to 3 months post-breach, c. 3 months post-breach to 9 months post-breach, and d. pre-breach to 9 months post-breach.

Planform changes

In addition to overall aggradation, reach 2 also exhibited post-breach changes in planform. By 1 week post-breach, photo analysis shows that the river began to deposit and rework bars in reach 2 from 4,550 m downstream to the river mouth. This resulted in an increase in bar area within reach 2 from 9,900 m^2 pre-breach to 24,700 m^2, and a decrease in wetted channel area from 152,000 to 137,200 m^2 (Figure 13, b.). By 3 months post-breach, bars in reach 2 continued to be reworked and approached a stable planform with 3 alternating lateral bars from 4,400 m downstream to the mouth (Figure 13, d.). Bar area increased to 71,200 m^2, the largest area measured in the study timeframe, and channel area decreased to 90,700 m^2, the smallest area measured in the study timeframe. Channel planform 9 months post-breach from 4,500 m downstream of the dam to the mouth mirrored the configuration established in 3 months post-breach with a lateral bar on river-right at the mouth, and a river-left lateral bar 600 m upstream (Figure 13, e). From 3,550 to 4,500 m downstream, the river braided and reworked the river-right lateral bar that was present 2 and 3 months post-breach. During this time, bar area in reach 2 decreased to 60,900 m^2 and the channel area increased to 100,900 m^2.

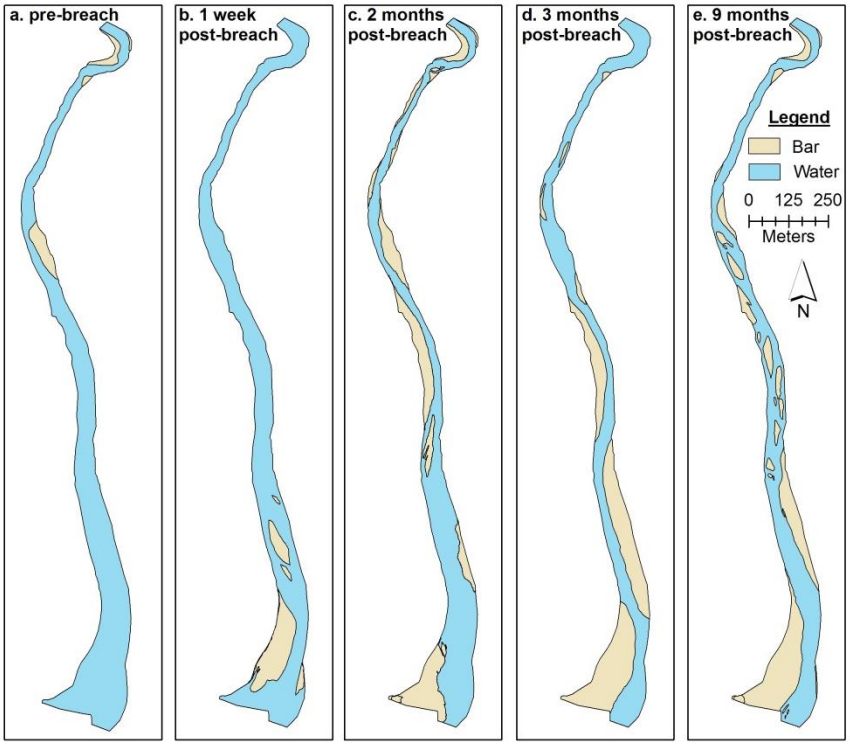

Figure 13: Digitized planform change in reach 2 from 2,850 m downstream of dam to the mouth. Bars shown in tan and water in blue. Alternating bars begin to form at mouth by 2 months post-breach and are still present by 9 months post-breach. Bar reworking and channel braiding seen from 3,650 to 4,100 m downstream at 9 months post-breach.

Changes in sediment storage

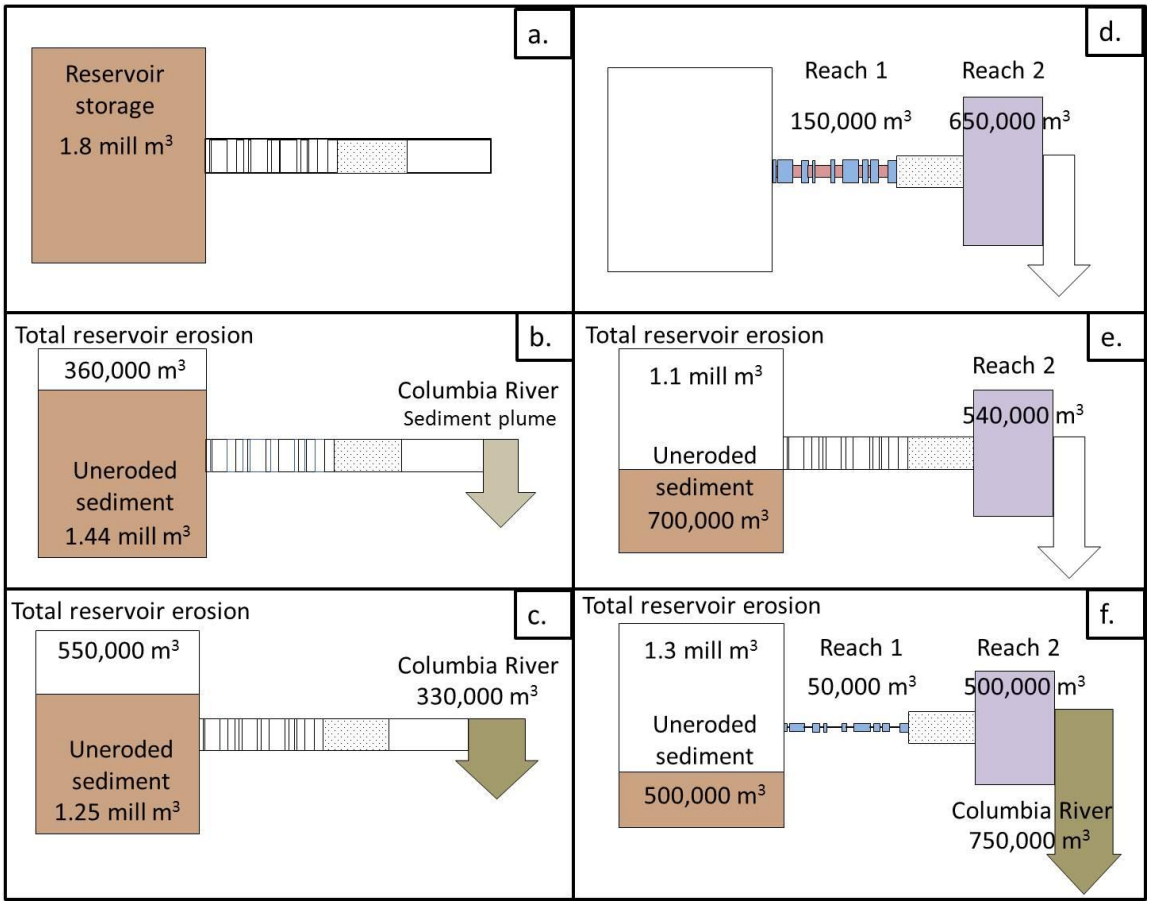

Figure 14: Changes in sediment storage volume in reservoir, pools and riffles in reach 1, reach 2, and the Columbia River. Increasing downstream distance from left to right, with grey area between reach 1 and 2 representing the portion of river not surveyed due to impassable conditions. Size of storage reservoirs varies in proportion to volume stored. Stored sediment in reservoir shown in brown, pools in blue, riffles in red, reach 2 in purple, and the Columbia River in tan. Unlabeled storage reservoirs indicate no data for that time period. Times shown include a) Pre-breach, b) 24 hours post-breach, c) 1 week post-breach, d) time of maximum bed aggradation (3 days to 3 weeks post-breach), e) 8 weeks post-breach, and f) 9 months post-breach.

Within 24 hours following the breach, 360,000 m^3, 20% of the total volume stored in the reservoir, had eroded from the reservoir and been transported downstream (Wilcox et al., 2014) (Figure 14, b). A plume of fine sediment in suspension began forming in the Columbia River at the mouth of the WSR (PacifiCorp Energy, 2011). By one week after the breach, 30% of the

reservoir sediment had eroded (Figure 14, c). Bathymetric surveys revealed that more than half of this eroded sediment had deposited in the Columbia River at the mouth of the WSR (PacifiCorp Energy, 2011). During the maximum aggradation of the sand bed within the first 3 weeks following the breach, reach 1 and 2 stored ~ 45% of the total reservoir sediment volume (Figure 14, d). Within reach 1, pools stored twice the volume of riffles. At the reach scale, reach 2 stored 4 times the volume of reach 1. By 8 weeks post-breach, ~ 60% of the initial reservoir sediment had eroded, and reach 2 stored half of this eroded sediment volume (Figure 14, e.). Over the next 7 months, an additional 10% of the initial reservoir sediment volume eroded (Figure 14, f.). By 9 months post-breach, ~ 30% of the pre-breach reservoir volume remained in place, reach 2 stored ~30%, and reach 1 stored < 5%.

The largest volume of sediment storage downstream occurred during the sand bed deposition, and pools and reach 2 continued to store more sediment than reach 1 and riffles by 9 months post-breach. At the time of sand bed deposition, the volume of sediment stored downstream of the dam was approximately 800,000 m^3, or 45% of the total pre-breach volume of reservoir sediment (Table 2). Pools stored 12% of this volume and riffles stored 6%, and reach 1 stored a cumulative 18% compared to the 82% stored in reach 2. By 9 months post-breach, the river stored less sediment than during sand bed conditions, and riffles and reach 1 showed the greatest reductions in stored sediment volume. At 9 months post-breach, the stored volume of sediment was approximately 550,000 m^3, or 2/3 of the sediment stored at the time of the sandy bed deposition and 29% of the pre-breach reservoir sediment volume (Table 2). Of the 550,000 m^3, reach 1 stored 10%, with pools and riffles storing 9 and 1% respectively, and reach 2 stored 90%.

Table 2: Volumes of sediment stored in reaches 1 and 2 and in pools and riffles from sand bed and 9 months post-breach conditions. Volumes rounded to the nearest thousand.

	Sediment volume at time of sand bed deposition (m^3)	**Percentage of total**	**Sediment volume 9 months post-breach (m^3)**	**Percentage of total**
Reach 1	150,000 ± 10,000	18	55,000 ± 5,000	10
Pools	100,000 ± 5,000	6	50,000 ± 15,000	9
Riffles	50,000 ± 5,000	12	5,000 ± 5,000	1
Reach 2	650,000 ± 10,000	82	500,000 ± 10,000	90
Total	800,000 ± 10,000		550,000 ± 15,000	

Changes in bed-material size

Pre-breach median grain sizes were coarsest near the dam (260 mm at 125 m downstream of the dam) and decreased in reach 1 with increasing distance from the dam (to 90 mm at 1,160 m downstream of the dam) (Figure 15). Post-breach sand deposits in reach 1 had a median grain size of 0.23 ± 0.05 mm with no discernible downstream fining. Four pebble counts performed 3 months post-breach in reach 1 showed D_{50} values between 55 to 80 mm, with no downstream trend (Figure 15). The mean (±standard deviation) of D_{50} values decreased from 143 ± 29 mm (pre-breach) to 66 ± 11 mm (3 months post-breach). By 9 months post-breach, median grain sizes ranged from 45 to 85 mm and were not significantly different from 3 months post-breach grain sizes. Post-breach grain size remained much finer than pre-breach values, with the coarsest 9 months post-breach median grain size (D_{50} = 85) still finer than the finest pre-breach grain size in reach 1 (D_{50} = 90).

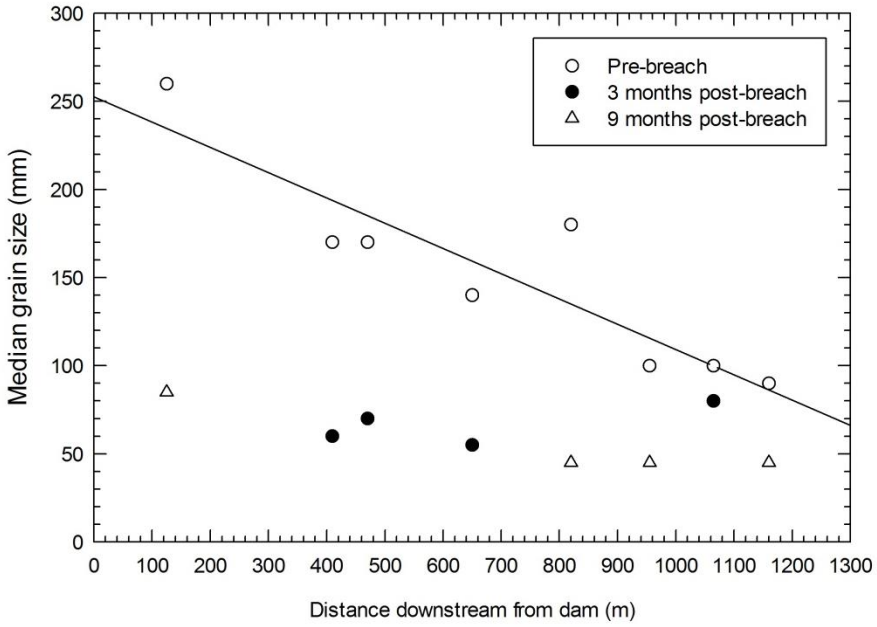

Figure 15: Median grain sizes from Wolman pebble counts in reach 1 for pre-breach, 3 months post-breach, and 9 months post-breach, illustrating post-breach fining. Pre-breach D_{50} decreases with increasing distance downstream, as indicated by the regression line ($R^2 = 0.82$); downstream trends are not evident among the 3 and 9 months post-breach D_{50} values.

Variations in transport capacity

Transport capacity, as calculated by bedload transport rate, showed downstream variations throughout reach 1 as a result of local changes in slope, channel width and depth, and grain size, as well as changes from the pre-breach to the 9-months post-breach condition. Pre-breach transport capacity varied from its lowest value at 125 m downstream from the dam to its maximum value at 1,150 m downstream (Figure 16). No consistent pattern of variation in transport capacity was evident between pre-breach and 9 months post-breach conditions, although local variations in the components of transport capacity are relevant. At 800 m downstream, a large decrease in grain size and increase in wetted width between pre-breach and 9 months post-breach likely drove the calculated increase in transport capacity here, and at

1,150 m downstream, the decrease in slope between pre-breach and 9 months post-breach drove the calculated decrease in transport capacity.

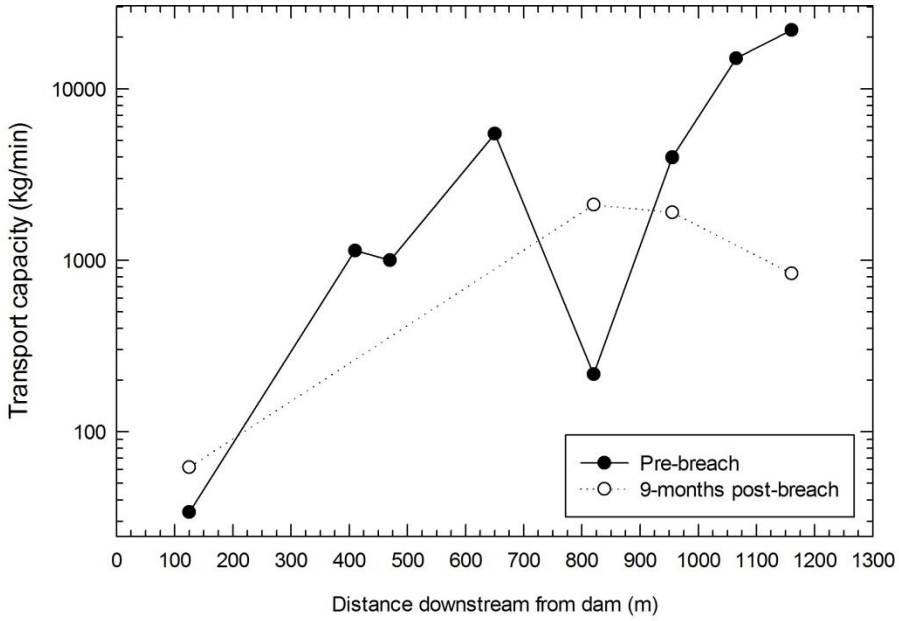

Figure 16: Downstream variations in transport capacity calculated for pre-breach and 9 months post-breach conditions from dam site to 1,300 m downstream.

DISCUSSION

Results support the prediction that riffles would exhibit a smaller magnitude and shorter duration of geomorphic adjustment than pools. The magnitude of bed elevation change from pre-breach to sand bed conditions was greatest over pools (Figure 10). Pools stored twice as much sediment during the initial bed aggradation as riffles, and, by 9 months post-breach, pools stored nine times as much sediment as riffles (Table 2). Nine months post-breach, pools and riffles incised the same amount on average, resulting in a faster rate of elevation change over riffles than pools. Between the 3 and 9 months post-breach surveys, the percentage of downstream sediment storage in pools decreased by 4% compared to the 7% reduction in riffles, demonstrating a longer duration of pool geomorphic adjustment. Results from the short-term aggradation of the sand bed are consistent with the pool infilling observed in previous dam removals, reservoir releases, and landslides (e.g. Madej, 1999; Major et al., 2012; Wohl and Cenderelli, 2000). However, by 9 months post-breach, riffles returned to within 1 m of their pre-breach elevations, while pools remained an average 2.2 m above pre-breach levels, indicating that bed incision had occurred in pools, but not to the extent as it had over riffles.

Further incision has likely occurred in pools beyond the 9 month time frame of this study. Thompson (2010) outlines a process of pool sediment evacuation and maintenance of pool-riffle bedforms whereby valley constrictions, large wood or boulders, or other lateral flow obstructions can reduce the active channel width and cause flows to converge in the center of the channel, increasing velocities and promoting pool scour (Thompson, Wohl, & Jarrett, 1999; Thompson, 2010). Rathburn and Wohl (2003) observed significant pool scour within the center of pools, but also noted that recirculation in eddies behind the lateral obstructions inhibits erosion and encourages deposition along channel edges.

Results also support the prediction that reach 1 would exhibit a smaller magnitude and shorter duration of geomorphic adjustment than reach 2. Kuo and Brierley (2013) reported similar findings in their assessment of sediment storage in the Liwu Basin, Taiwan. They found limited sediment storage in the confined reaches that occupy 82% of the basin area, and found that relatively short, unconfined reaches store 95% of the basin sediment volume (Kuo & Brierley, 2013).

I propose that the patterns of sediment storage and transport observed in bedforms and reaches can be explained by a conceptual model of changes in sediment supply and transport capacity following the dam breach (Figure 17). An increase in sediment supply can cause an increase in bedload transport, storage, or bed fining (e.g. Lisle and Hilton, 1992; Montgomery and Buffington, 1997; Rathburn and Wohl, 2003), and the WSR displayed all of these responses. The initial deposition over pools and riffles and subsequent bed aggradation was due to the sediment supply from the breach greatly exceeding the transport capacity of the bedforms. However, the sediment deposited was much finer than the gravels and cobbles that mountain rivers typically transport, and so, once the initial increase in sediment supply caused by massive reservoir erosion in the first weeks subsided, transport capacity exceeded supply and resulted in bed incision.

Pool infilling and fining of the bed likely produced feedbacks that contributed to sediment evacuation from reach 1 after the initial sand bed deposition. A decrease in grain size reduces the critical shear stress needed to mobilize sediments, thus enhancing sediment transport (Lisle, 1982). Bed fining also smooths the bed surface and reduces hydraulic roughness associated with skin friction (Venditti et al., 2010), increasing the effective shear stress that can be used for transport (Montgomery & Buffington, 1997). The dam removal also altered hydraulic roughness from bedforms. When the abrupt slope changes of pool-riffle

bedforms are masked by pool-infilling, roughness decreases and an increase in transport can occur, and these changes in channel from and grain size may have contributed to post-breach transport from reach 1 and storage in reach 2.

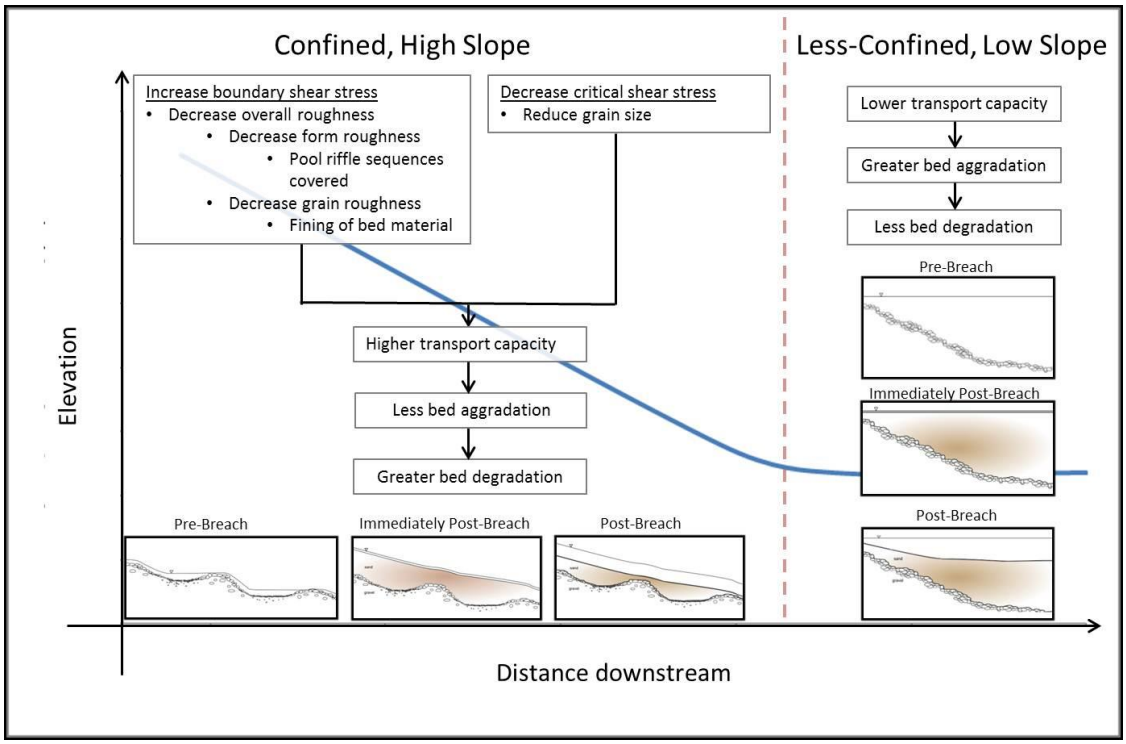

Figure 17: Conceptual model of downstream response to sediment disturbance on the WSR. Initial deposition of fine reservoir sediment in reach 1 (confined, high slope) led to a decrease in critical shear stress from grain size fining and an increase in boundary shear stress due to a decrease in form and grain roughness. These changes promoted transport from reach 1 and promoted greater bed degradation or incision. The less-confined, low slope conditions in reach 2 resulted in a lower transport capacity and promoted long-term sediment storage.

My observation that large magnitudes and durations of change occurred where the WSR shifts from a high to low transport-capacity reach, as the sediment transported from upstream accumulates at the entrance to the low-transport reach, is consistent with other studies of channel response to sediment disturbance (Montgomery & Buffington, 1997; Podolak & Wilcock, 2013). At the upstream end of reach 2, around 3,150 m downstream of the dam site, the channel slope rapidly decreases and valley width increases, reducing transport capacity.

Sediment accumulation here caused dynamic changes in WSE (reflecting changes in bed elevation) and planform. The gradient in elevation changes between the pre-breach and 2 and 9 month post-breach profiles suggest the deposition and downstream transport of wedge of sediment between 3,150 and 4,800 m downstream of the dam site (Figure 4). Major et al. (2012) also observed the deposition a sediment wedge on the Sandy River reach immediately downstream of Marmot Dam. By 1 month after the Marmot Dam breach, the wedge stored 50% of the total eroded reservoir sediment, and continued to store 25% of the total eroded sediment 2 years later (Major et al., 2012). In their flume experiment assessing the impact of increased sediment supply to a gravel bed channel, Podolak and Wilcock (2013) also observe the deposition of a sediment wedge and the continued reworking of bars and surface texture. In the WSR, planform and GCD results also reveal similar bar deposition and braiding in the upstream portion of reach 2 (Figures 11 and 12).

Results from the initial sand bed aggradation and subsequent incision within the first 3 weeks following the breach provide evidence for dispersion and translation of bed sediment. From the dam site to 1,200 m downstream, the magnitude of bed elevation change over pools and riffles decreases with increasing distance from the dam. Pizzuto (2002) observes similar trends from flume and field studies of downstream geomorphic response to sediment disturbance and claims that dispersion of sediment from its original source explains this pattern of response. Lisle (2008) adds that sediment pulses where grain size is much finer than the pre-disturbance bed promote translation of sediment impacts where the locus of bed aggradation and incision moves downstream, as seen within the initial sand bed aggradation in the WSR.

Transport capacity calculations reveal the impacts that local changes in channel and water surface slope, wetted width, and grain size can have on the magnitude and duration of response. Deposition in the pools and riffles within the first 1,200 m downstream of the dam

caused a reduction in grain and bedform roughness and contributed to an increase in transport, as did the increase in wetted width within this reach. However, the increase in discharge and deposition in this reach also reduced water surface slopes, and the interplay between slope, grain size, and channel width determined the transport capacity calculated over riffles.

Local changes in transport capacity may also be driven by large wood deposition, as shown in the WSR by profile results from 1,200 to 1,500 m downstream of the dam (Figure 4) and observations of wood accumulation in this reach (Figure 9). The highly-confined nature of this reach caused the accumulation of wood and cut logs released during the breach. This reach had also intermittently accumulated log jams prior to the dam breach. Studies in mountain rivers have documented the tendency of channels to store large wood and the resulting local sediment storage upstream of the jam and scour downstream (Hassan et al., 2008; Montgomery & Buffington, 1997). Profile elevation changes in this reach suggest that the jam developed before the 2 months post-breach survey, and the amount of sediment trapped upstream from the jam grew between the 2 to 9 months post-breach surveys (Figure 4). In the fall of 2012, contractors removed the log jam to reduce boating hazards, likely resulting in sediment evacuation from this reach and shifting of bed elevations toward pre-breach levels.

The abrupt nature of the Condit Dam breach and the unique, nested channel morphology exerted the largest controls on downstream geomorphic response. The dam breach caused mass wasting of reservoir sediments and rapidly introduced large amounts of fine sediment downstream. Within 1 week after the breach, 30% of the reservoir sediment volume had been evacuated. In comparison, within 2 weeks after the sudden breach of the Marmot Dam from the Sandy River, OR in 2007, only 15% of reservoir sediment had been eroded and transported downstream (Major et al., 2012). In the WSR, differing reach morphologies resulted in the greatest magnitude and duration of geomorphic impacts occurring over 3,000 m

downstream from the dam site in reach 2. Within the otherwise high-transport reach 1, pools provided significant storage reservoirs. Although reservoir erosion was slower, reach and bedform morphology also played a dominant role in the downstream geomorphic response to the Marmot Dam removal in 2007. Here, significant deposition occurred in a low gradient reach immediately downstream of the dam, and pools provided sediment storage in an otherwise high-transport gorge reach (Major et al., 2012).

Dam removals such as Condit can produce a combination of short-term, negative impacts and long-term benefits to aquatic habitat. Negative impacts to aquatic habitat caused by dam removals include shallower pools, which result in less resting, overwintering, and rearing fish habitat, fine sediment deposition on gravels, which reduces spawning sites and altering macroinvertebrate populations, and the overall reduction of channel and habitat complexity caused by large-scale deposition (Downs et al., 2009; Rathburn & Wohl, 2003; Wohl & Cenderelli, 2000). Over time, positive changes resulting from dam removals include the return of the natural flow regime and associated ecosystem processes, restored access to upstream habitat, and an increase in channel complexity resulting from upstream influxes of organic matter and large wood (Downs et al., 2009). In the WSR, US Fish and Wildlife surveys in the fall of 2012, one year post-breach, revealed fall Chinook Salmon redds from 2,100 m downstream of the dam to the mouth and at 3,900 m upstream of the dam (Engle, Skalicky, Poirier, Fish, & Service, 2012).

Channel recovery from a sediment disturbance can be assessed using both ecological and physical metrics. For example, Gardner et al. (2013) use fish density, biomass amounts, and species richness and diversity from a reference stream to assess channel recovery from two low-head dam removals in Maine. Physical metrics, such as the return to pre-disturbance bed

elevations and channel geometry, can provide another measure of recovery (Madej et al., 2009). However, if a disturbance is catastrophic, the channel may not return to pre-disturbance form (Madej et al., 2009; Montgomery & Buffington, 1997). Lisle and Hilton (1992) suggest that a channel may have recovered from disturbance when the balance of sediment supply and transport capacity results in no net erosion or deposition over time. Nine months post-breach in the WSR, bed elevations in pools and reach 2 had not returned to pre-breach levels. The time-frame of my study is too short to accurately assess long-term channel evolution. The low transport capacity in reach 2 and the continued accumulation of sediment in this reach suggest that bed elevations will not return to pre-breach levels, and that a new channel form will result when sediment supply and transport capacity have balanced.

CONCLUSION

The Condit Dam breach on the WSR provided an exceptional environment in which to study downstream geomorphic response to a large influx of fine sediment. Results show that riffles and the confined, high-gradient reach 1 exhibited a smaller magnitude and duration of geomorphic adjustment than pools and the less-confined, low-gradient reach 2. I propose a conceptual model of geomorphic response in the WSR in which the reduction of grain size and form and grain roughness enhances sediment transport from reach 1 to reach 2. The transition from reach 1 to reach 2, and reach 2 in general, exhibited dynamic, long-lasting change. The removal of Condit Dam increased access to aquatic habitat and observations showed fish spawning upstream from the dam site within one year after the breach. The geomorphic response of the WSR to the Condit Dam breach can inform future dam removal methods and expected downstream geomorphic response to sediment disturbance.

REFERENCES

American Rivers. (2012). *http://www.americanrivers.org/assets/pdfs/dam-removal-docs/dams-removed-1998-to-2012.pdf*.

Barnes, H. (1967). Roughness Characteristics of Natural Channels. *U.S. Geol. Surv. Prof. Pap. 1849*.

Bountry, J. A., Lai, Y. G., & Randle, T. J. (2013). Sediment impacts from the Savage Rapids Dam removal, Rogue River, Oregon. *Reviews in Engineering Geology*, *21*, 93–104.

CH2M HILL. (2002). *Evaluation of Condit Hydroelectric Project as a Power Supply Resource*. Letter to Klickitat County Public Utility District.

Cui, Y., & Wilcox, A. (2008). Development and application of numerical models of sediment transport associated with dam removal. In *Sedimentation Engineering: Theory, Measurements, Modeling, and Practice, ASCE Manual 110*. Garcia, M.H., ed., 995-1020, ASCE, Reston, VA.

Czuba, C. R., Randle, T. J., Bountry, J. A., Christopher, S., Czuba, J. A., Christopher, A., & Konrad, C. P. (2011). Anticipated Sediment Delivery to the Lower Elwha River During and Following Dam Removal. In *Coastal Habitats of the Elwha River, Washington—Biological and Physical Patterns and Processes Prior to Dam Removal*. Duda, J. J. Warrick, J. A., & Magirl, C. S., eds., 27-46.

Downs, P. W., Cui, Y., Wooster, J. K., Dusterhoff, S. R., Derek, B., Dietrich, W. E., & Sklar, L. S. (2009). Managing reservoir sediment release in dam removal projects : An approach informed by physical and numerical modelling of non- cohesive sediment. *Intl. J. River Basin Management*, *7*(4), 443–452.

Doyle, M. W., Stanley, E. H., & Harbor, J. M. (2002). Geomorphic analogies for assessing probable channel response to dam removal. *Journal Of The American Water Resources Association*, *38*(6), 1567–1579.

Doyle, M. W., Stanley, E. H., Harbor, J. M., & Grant, G. S. (2003). Dam removal in the United States: Emerging needs for science and policy. *Eos, Transactions American Geophysical Union*, *84*(4), 29.

Engle, R., Skalicky, J., Poirier, J., Fish, U. S., & Service, W. (2012). *Translocation of Lower Columbia River Fall Chinook Salmon (Oncorhynchus tshawytscha) In the Year of Condit Dam*

Removal and Year One Post-Removal Assessments. U.S. Fish and Wildlife Service, Vancouver, WA.

ESSA Technologies, North Arrow Research, & Wheaton, J. (2012). *Geomorphic Change Detection 5.0 software*.

Evans, E., & Wilcox, A. C. (2014). Fine sediment infiltration dynamics in a gravel-bed river following a sediment pulse. *River Research and Applications*, *30*(3), 372–384.

Gardner, C., Coghlan Jr., S., Zydlewski, J., & Saunders, R. (2013). Distribution and abundance of stream fishes in relation to barriers: implications for monitoring stream recovery after barrier removal. *River Res. Applic.*, *29*, 65–78.

Gran, K. B., & Montgomery, D. R. (2005). Spatial and temporal patterns in fluvial recovery following volcanic eruptions: Channel response to basin-wide sediment loading at Mount Pinatubo, Philippines. *Geological Society of America Bulletin*, *117*(1), 195.

Hassan, M. A., Smith, B. J., Hogan, D. L., Luzi, D. S., Zimmermann, A. E., & Eaton, B. C. (2008). Sediment storage and transport in coarse bed streams: scale considerations. In *Gravel-Bed Rivers VI: From Process Understanding to River Restoration*. H. Habersack, H. Piegay, M. Rinaldi, eds., 473-496, Elsevier B.V.

Konrad, C. P. (2009). Simulating the recovery of suspended sediment transport and river-bed stability in response to dam removal on the Elwha River, Washington. *Ecological Engineering*, *35*(7), 1104–1115.

Kuo, C. W., & Brierley, G. J. (2013). The influence of landscape configuration upon patterns of sediment storage in a highly connected river system. *Geomorphology*, *180-181*, 255–266.

Lisle, T. E. (1982). Effects of Aggradation and Degradation on Riffle-Pool Morphology in Natural Gravel Channels , Northwestern California. *Water Resources Research*, *18*(6), 1643–1651.

Lisle, T. E. (2008). The evolution of sediment waves influenced by varying transport capacity in heterogeneous rivers. In *Gravel-Bed Rivers VI: From Process Understanding to River Restoration*. H. Habersack, H. Piegay, & M. Rinaldi, eds., 443-472, Elsevier B.V.

Lisle, T. E., & Hilton, S. (1992). the Volume of Fine Sediment in Pools: an Index of Sediment Supply in Gravel-Bed Streams. *Journal of the American Water Resources Association*, *28*(2), 371–383.

Madej, M. (1999). Temporal and spatial variability in thalweg profiles of a gravel-bed river. *Earth Surface Processes and Landforms*, *24*, 1153–1169.

Madej, M. A., Sutherland, D. G., Lisle, T. E., & Pryor, B. (2009). Channel responses to varying sediment input: A flume experiment modeled after Redwood Creek, California. *Geomorphology*, *103*(4), 507–519.

Magirl, C. S., Connolly, P. J., Coffin, B., Duda, J. J., Curran, C. A., & Draut, A. E. (2010). Sediment management strategies associated with dam removal in the State of Washington. In *Proceedings of the 2nd Joint Federal Interagency Conference*. J.M. Bernard and J.W. Webb, eds., Las Vegas, NV.

Major, J. J., O'Connor, J. E., Podolak, C. J., Keith, M. K., Grant, G. E., Spicer, K. R., … Wilcock, P. R. (2012). Geomorphic Response of the Sandy River, Oregon, to Removal of Marmot Dam. *U.S. Geol. Surv. Prof. Pap. 1792*, 76.

Montgomery, D., & Buffington, J. (1997). Channel-reach morphology in mountain drainage basins. *Bulletin of the Geological Society of America*, *109*(5), 596–611.

Mosley, M. P., & McKerchar, A. I. (1993). Streamflow. In *Handbook of Hydrology*. D.R. Maidment, ed., 1-39, McGraw-Hill, New York.

PacifiCorp Energy. (2002). History of the Condit Hydroelectric Project. Prepared by EDAW, Inc.

PacifiCorp Energy. (2006). *Condit Dam and Northwestern Lake Hydrographic Surveys Final Report*. Prepared by Finley Engineering.

PacifiCorp Energy. (2011). 90 day preliminary sediment behavior report. FERC Project No. 2342, Prepared by Riverbend Engineering, LLC and JR Merit.

PacifiCorp Energy. (2012). *120 day post-reservoir-dewatering assessment report*. Prepared by Riverbend Engineering, LLC and J.R. Merit.

Pitlick, J., Cui, Y., & Wilcock, P. (2009). *Manual for Computing Bed Load Transport Using BAGS (Bedload Assessment for Gravel-bed Streams) Software*.

Pizzuto, J. (2002). Effects of dam removal on river form and process. *BioScience*, *52*(8), 683–691.

Podolak, C. J. P., & Wilcock, P. R. (2013). Experimental study of the response of a gravel streambed to increased sediment supply. *Earth Surface Processes and Landforms*, *38*(14), 1748–1764.

Rathburn, S., & Wohl, E. E. (2003). Predicting fine sediment dynamics along a pool-riffle mountain channel. *Geomorphology*, *55*, 111–124.

Sawaske, S. R., & Freyberg, D. L. (2012). A comparison of past small dam removals in highly sediment-impacted systems in the U.S. *Geomorphology*, *151-152*, 50–58.

Thompson, D. M. (2010). The velocity-reversal hypothesis revisited. *Progress in Physical Geography*, *35*(1), 123–132.

Thompson, D. M., Wohl, E. E., & Jarrett, R. D. (1999). Velocity reversals and sediment sorting in pools and riffles controlled by channel constrictions. *Geomorphology*, *27*, 229–241.

Tullos, D., & Wang, H. W. (2014). Morphological responses and sediment processes following a typhoon-induced dam failure, Dahan River, Taiwan. *Earth Surface Processes and Landforms*, *39*(2), 245–258.

Venditti, J. G., Dietrich, W. E., Nelson, P. a., Wydzga, M. a., Fadde, J., & Sklar, L. (2010). Effect of sediment pulse grain size on sediment transport rates and bed mobility in gravel bed rivers. *Journal of Geophysical Research*, *115*, 1–19.

Walter, C., & Tullos, D. D. (2010). Downstream channel changes after a small dam removal: Using aerial photos and measurement error for context; Calapooia River, Oregon. *River Res. Applic.*, *26*(10), 1220–1245.

Washington State Dept of Ecology. (2007). Condit Dam Removal Final SEPA Supplemental Environmental Impact Statement. Ecology Publication # 07-06- 0.

Watershed Sciences Inc. (2012). *Condit Dam, Washington LiDAR data*. Corvallis, OR.

Wilcock, P., Pitlick, J., & Cui, Y. (2009). *Sediment Transport Primer: Estimating Bed-Material Transport in Gravel-bed Rivers*. USDA Forest Service Rocky Mountain Research Station, General Technical Report 226.

Wilcox, A. C., Connor, J. E. O., & Major, J. J. (2014). Rapid reservoir erosion, hyperconcentrated flow, and downstream deposition triggered by breaching of 38 m tall Condit Dam, White Salmon River, Washington. *Journal of Geophysical Research: Earth Surface*, *119*(6), 1376–1394.

Wohl, E. (2010). *Mountain Rivers Revisited*. American Geophysical Union, Water Resources Monograph Series, Volume 19, 573.

Wohl, E. (2011). Threshold-induced complex behavior of wood in mountain streams. *Geology*, *39*(6), 587–590.

Wohl, E.E., & Cenderelli, D. A. (2000). Sediment deposition and transport patterns following a reservoir sediment release. *Water Resources Research*, *36*(1), 319–333.

Wohl, Ellen E., Thompson, D. M., & Miller, A. J. (1999). Canyons with undulating walls. *Geological Society of America Bulletin*, *111*(7), 949–959.

Wolman, M. G. (1954). A method of sampling coarse river-bed material. *Trans. Am. Geophys. Union*, *35*, 951–956.

APPENDIX A: CROSS SECTIONS

Surveyed cross sections from White Salmon River downstream of dam site. Data availability varies as a result of variations in flow and wadeability and include surveys from pre-breach, 3-months post-breach, and 9-months post-breach.

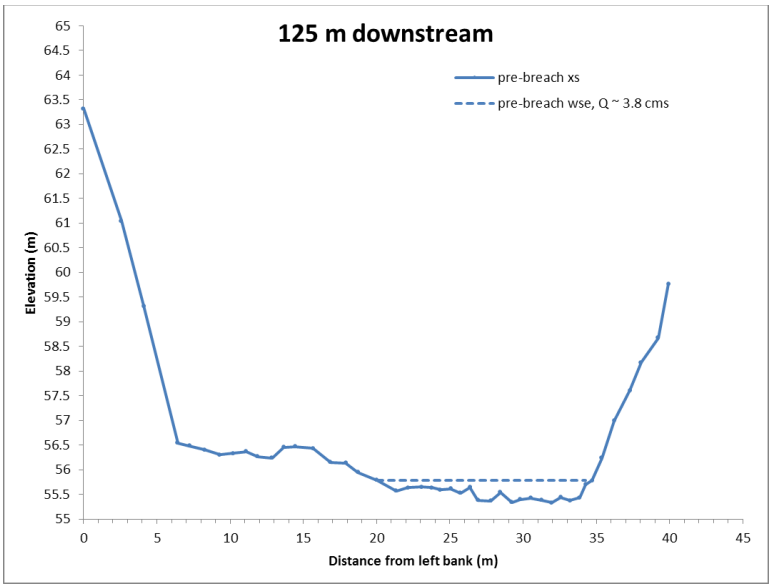

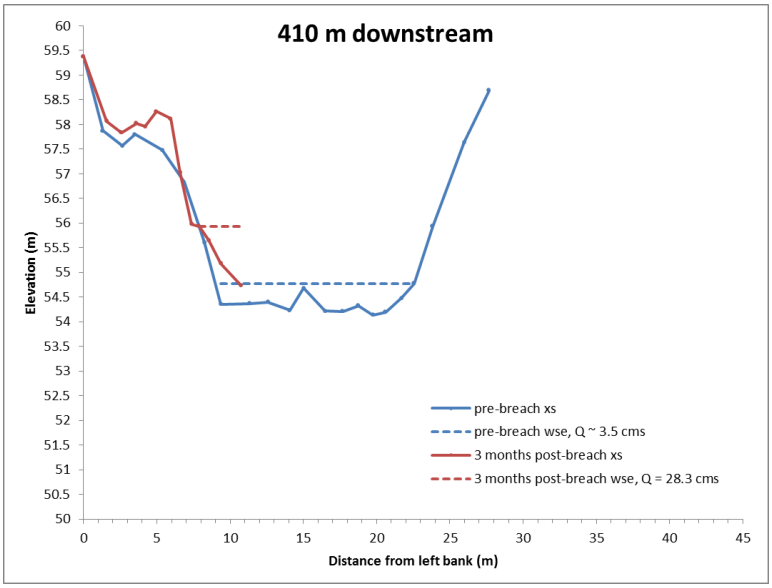

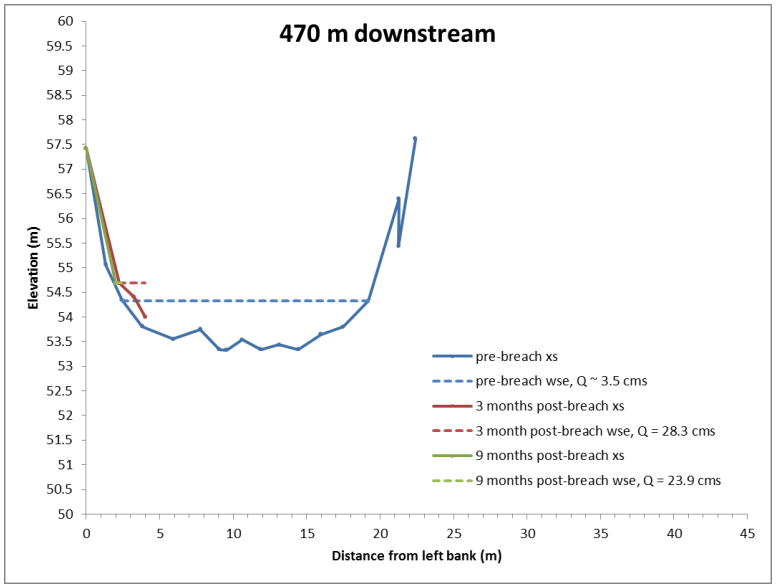
470 m downstream
Elevation (m)
Distance from left bank (m)
pre-breach xs
pre-breach wse, Q ~ 3.5 cms
3 months post-breach xs
3 month post-breach wse, Q = 28.3 cms
9 months post-breach xs
9 months post-breach wse, Q = 23.9 cms

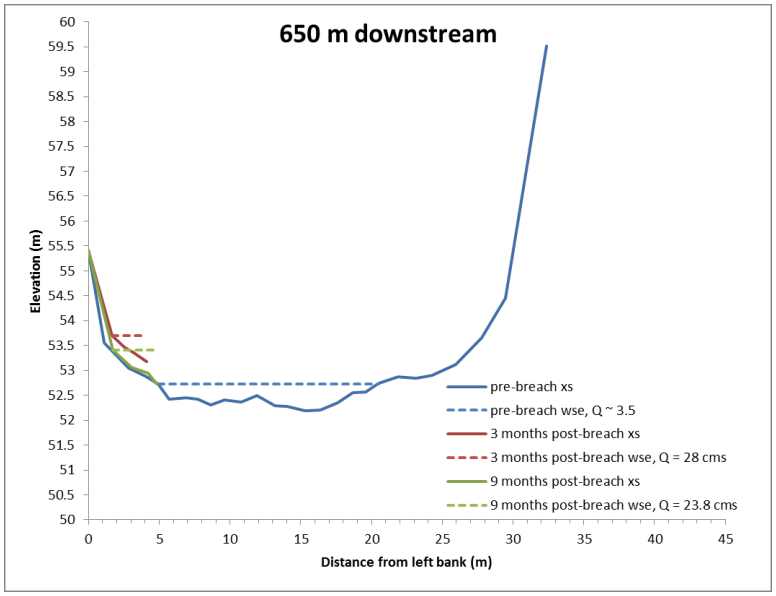
650 m downstream
Elevation (m)
Distance from left bank (m)
pre-breach xs
pre-breach wse, Q ~ 3.5
3 months post-breach xs
3 months post-breach wse, Q = 28 cms
9 months post-breach xs
9 months post-breach wse, Q = 23.8 cms

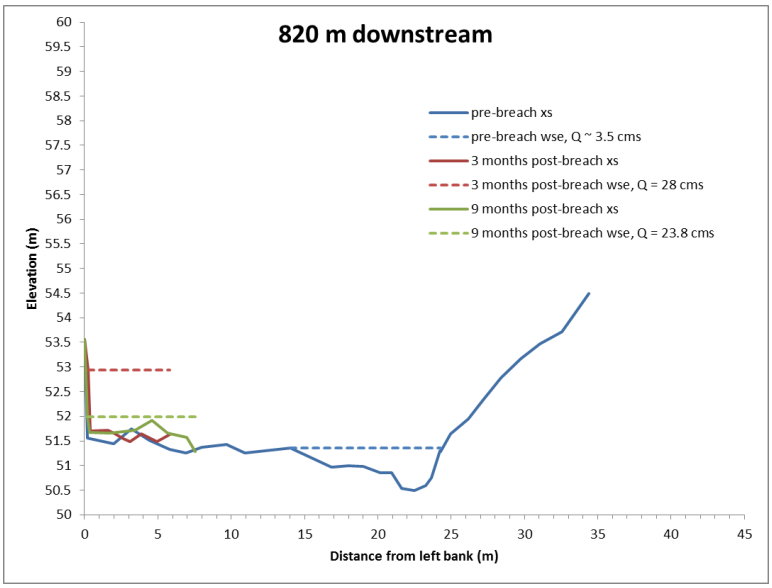
820 m downstream
Elevation (m)
Distance from left bank (m)
pre-breach xs
pre-breach wse, Q ~ 3.5 cms
3 months post-breach xs
3 months post-breach wse, Q = 28 cms
9 months post-breach xs
9 months post-breach wse, Q = 23.8 cms

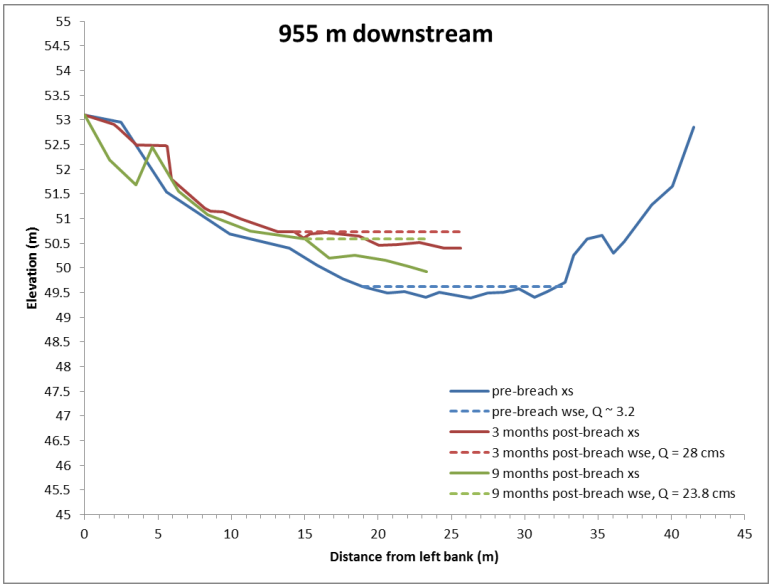
955 m downstream
Elevation (m)
Distance from left bank (m)
pre-breach xs
pre-breach wse, Q ~ 3.2
3 months post-breach xs
3 months post-breach wse, Q = 28 cms
9 months post-breach xs
9 months post-breach wse, Q = 23.8 cms

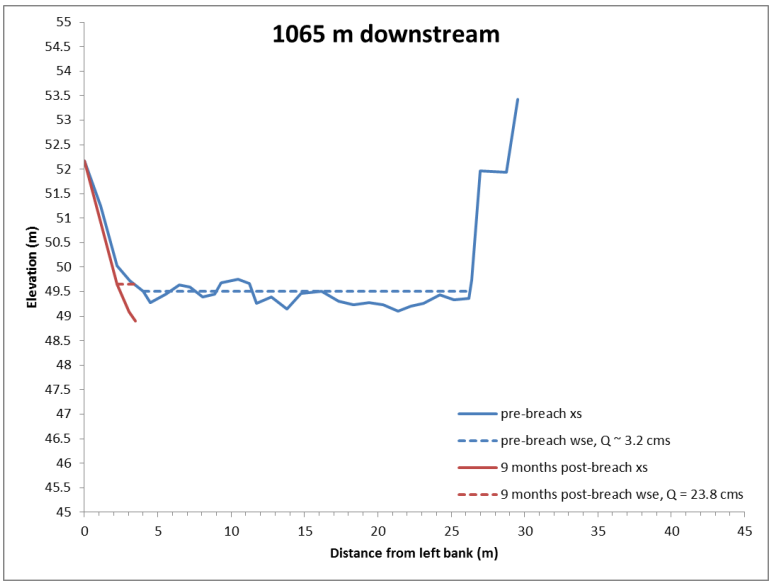
1065 m downstream
Elevation (m)
Distance from left bank (m)
pre-breach xs
pre-breach wse, Q ~ 3.2 cms
9 months post-breach xs
9 months post-breach wse, Q = 23.8 cms

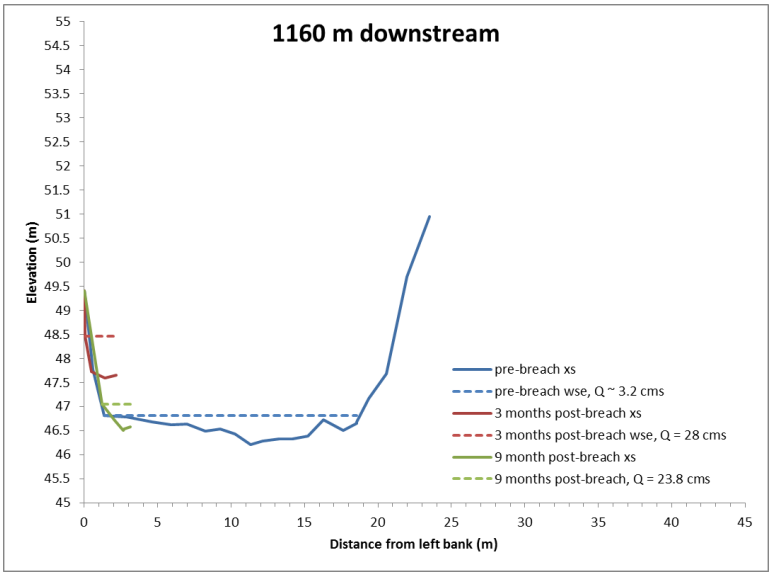
1160 m downstream
Elevation (m)
Distance from left bank (m)
pre-breach xs
pre-breach wse, Q ~ 3.2 cms
3 months post-breach xs
3 months post-breach wse, Q = 28 cms
9 month post-breach xs
9 months post-breach, Q = 23.8 cms

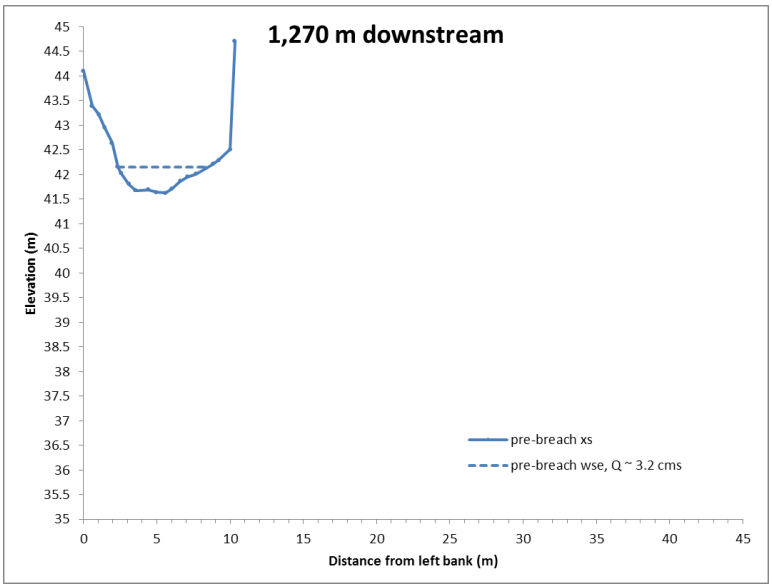
1,270 m downstream
Elevation (m)
Distance from left bank (m)
pre-breach xs
pre-breach wse, Q ~ 3.2 cms

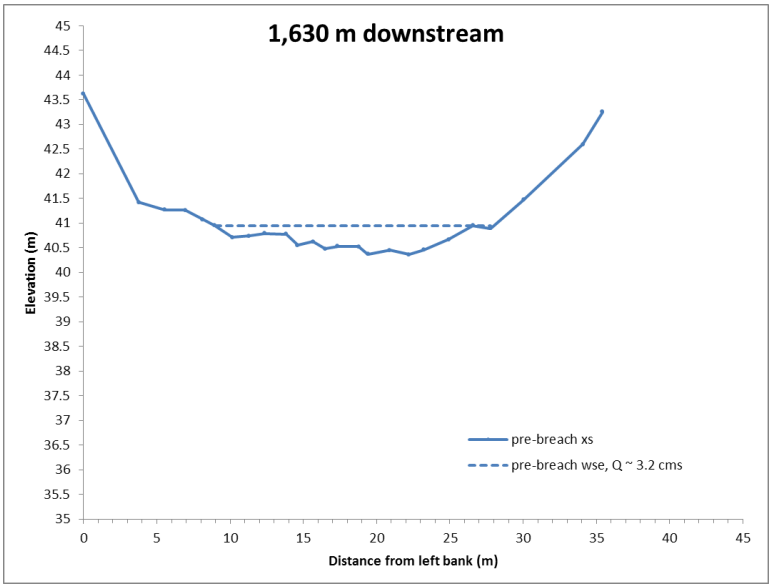
1,630 m downstream
Elevation (m)
Distance from left bank (m)
pre-breach xs
pre-breach wse, Q ~ 3.2 cms

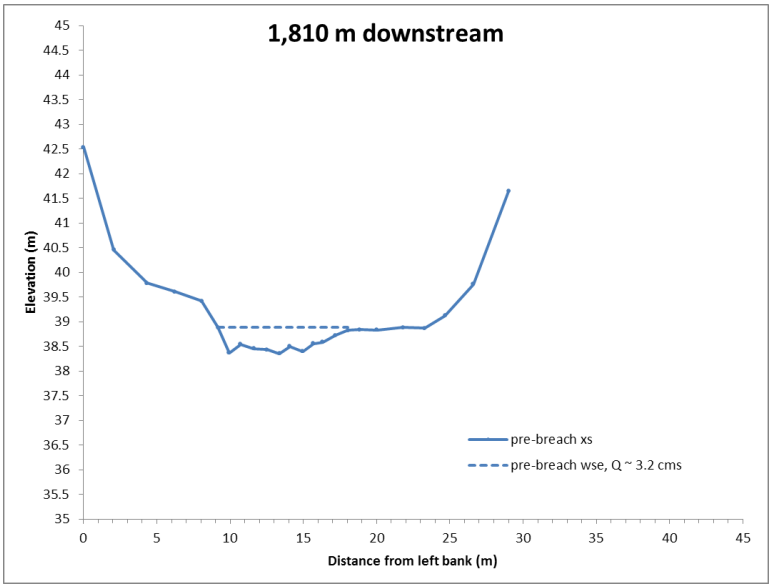
1,810 m downstream
Elevation (m)
Distance from left bank (m)
pre-breach xs
pre-breach wse, Q ~ 3.2 cms

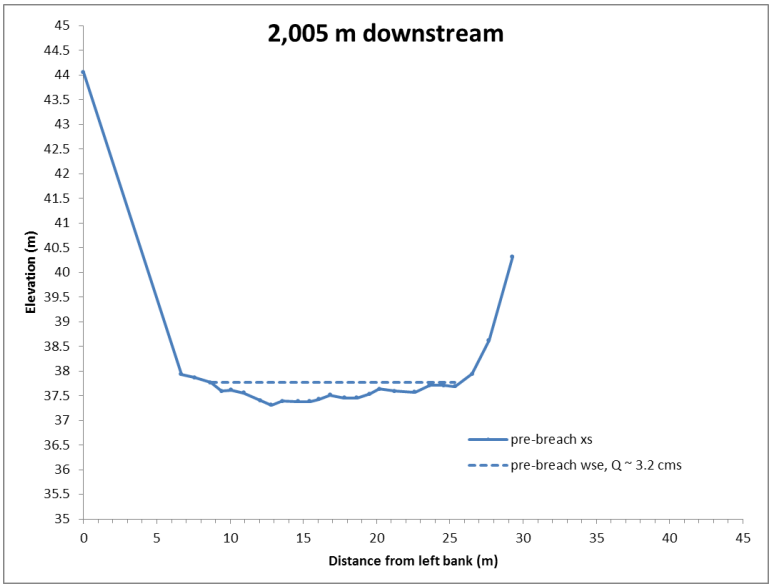
2,005 m downstream
Elevation (m)
Distance from left bank (m)
pre-breach xs
pre-breach wse, Q ~ 3.2 cms

APPENDIX B: FIELD PHOTOGRAPHY

Additional field photography, specific to aggraded sand-bed deposits, is shown in Appendix G.

Photos of typical pre-breach pools and riffles, taken August 2011:

Photograph taken on August 6, 2011 at 150 m downstream of dam.

Photograph taken on August 6, 2011 at 700 m downstream of dam.

The following photographs show cross section survey locations and are taken from the left bank looking across the channel.

125 m downstream of dam:

3 months post-breach

9 months post-breach

400 m downstream of dam:

pre-breach

3 months post-breach

9 months post-breach

475 m downstream of dam:

pre-breach

3 months post-breach

650 m downstream of dam:

pre-breach

9 months post-breach

820 m downstream of dam:

pre-breach

3 months post-breach

9 months post-breach

955 m downstream of dam:

pre-breach

3 months post-breach

1,050 m downstream of dam:

pre-breach

3 months post-breach

9 months post-breach

1,150 m downstream of dam:

pre-breach

3 months post-breach

9 months post-breach

APPENDIX C: POOL BATHYMETRY

2.5 m-resolution DEMs developed from pre-breach pool depth points surveyed August 2011.

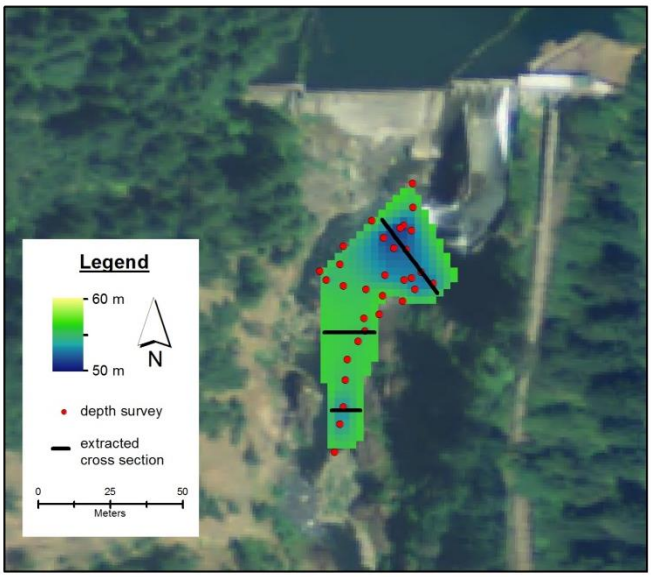

Pre-breach pool bathymetry, extending 0 - 110 m downstream of dam.

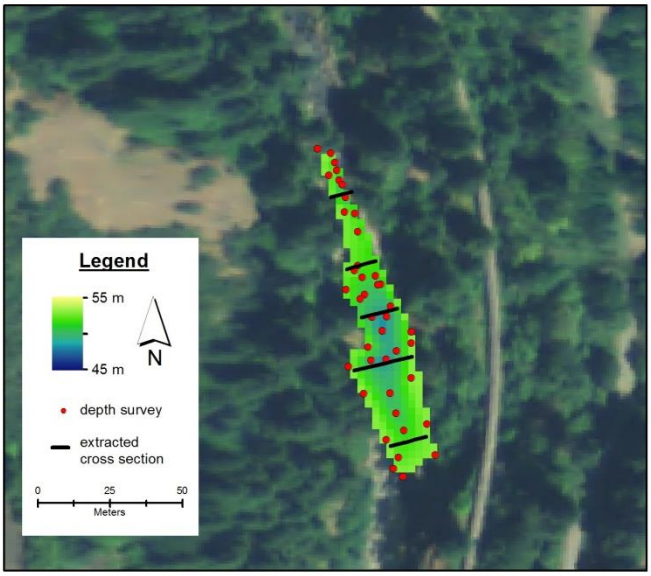

Pre-breach pool bathymetry, extending 480 - 610 m downstream of dam.

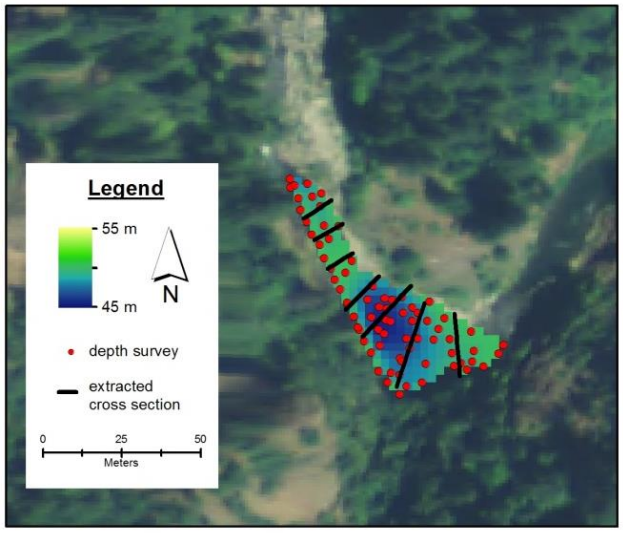

Pre-breach pool bathymetry, extending 850 - 930 m downstream of dam.

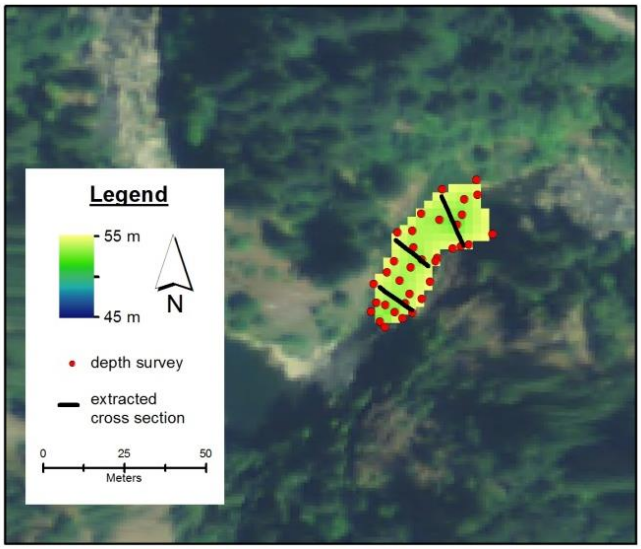

Pre-breach pool bathymetry, extending 970 – 1020 m downstream of dam.

APPENDIX D: AUGUST 2012 DEPTH CALCULATIONS

Calculations over pools

dist ds (m)	date	time (s)	Length (m)	U (m/s)	U*0.86 (m/s)	avg daily Q (cms)	xs area (cms / Q) (sq. m)	width (m)	depth (m)
280	8/6/2012	83.32	218.73	2.67	2.29	24.24	10.57	12.43	1.08
		82.20							
		78.37							
		83.60							
		82.72							
		avg time (s)						avg width (m)	
		82.04						12.43	
545	8/7/2012	53.76	112.00	2.16	1.86	23.79	12.81	19.13	0.85
		56.07						19.40	
		48.95							
		51.47							
		49.06							
		avg time (s)						avg width (m)	
		51.86						19.27	
715	8/7/2012	18.85	37.60	1.70	1.47	23.79	16.23	19.33	0.94
		18.03						25.44	
		21.11						21.07	
		20.30							
		32.01							
		avg time (s)						avg width (m)	
		22.06						21.94	
890	8/8/2012	18.53	30.33	1.89	1.62	23.76	14.65	15.80	0.97
		13.54						18.30	
		15.09						23.88	
		17.42						19.33	
		15.84							
		avg time (s)						avg width (m)	
		16.08						19.33	

995	8/8/2012	32.78	53.50	1.82	1.56	23.76	15.20	22.12	0.87
		33.24							
		26.92							
		27.45							
		26.78							
		avg time (s)						avg width (m)	
		29.43						22.12	
1,900	8/16/2012	62.74	122.00	1.87	1.61	21.75	13.52	15.30	0.95
		64.42						21.00	
		64.04						18.15	
		65.23							
		69.72							
		avg time (s)						avg width (m)	
		65.23						18.15	

Riffle velocities and depth

dist ds (m)	date	time (s)	Length (m)	U (m/s)	U*0.86 (m/s)	avg daily Q (cms)	xs area (cms / Q) (sq. m)	width (m)	depth (m)
125	8/6/2012	8.35	24.44	3.16	2.72	24.24	8.91	31.68	0.40
		8.33						25.48	
		6.54							
		8.29							
		7.12							
		avg time (s)						avg width (m)	
		7.726						28.58	
440	8/6/2012	36.28	105.57	2.91	2.50	24.24	9.70	16.29	0.75
		31.93						13.46	
		35.57						14.29	
		33.69						19.13	
		44.22						18.93	
		36.338							
		avg time (s)						avg width (m)	
		36.338						16.42	
650	8/7/2012	15.75	48.15	2.70	2.32	23.79	10.26	24.15	0.64
		16.33						17.32	
		20.82						19.33	
		15.57						20.27	
		20.81							
		avg time (s)						avg width (m)	
		17.856						20.27	
820	8/8/2012	50.11	142.5	2.62	2.25	23.76	10.54	26.70	0.49
		56.97						27.46	
		56.54						28.09	
		53.94							
		60.86							
		47.85							
		avg time (s)						avg width (m)	
		54.37833333						27.41	

APPENDIX E: DATA USED IN BAGS TRANSPORT CALCULATION

	August 2011			August 2012			
distance downstream	bedload transport (kg/min)	slope	mannings n	bedload transport (kg/min)	slope	wetted width (m)	mannings n
125	34	0.01552084	0.065	62	0.008547	28.58 m	0.06
410	1142	0.018152745	0.075				
470	1001	0.018385636	0.075				
650	5472	0.023470453	0.065				
820	216	0.014969839	0.075	2108	0.013137	27.41466667	0.06
955	3983	0.017689077	0.06	1900	0.011582	23.89	0.06
1065	15094	0.03455972	0.075				
1160	22004	0.032469102	0.075	840	0.009967	19.20525	0.07

APPENDIX F: BONNEVILLE POOL LEVELS

To assess the impact of Bonneville pool elevation fluctuations on reach 2, I plotted and compared average daily Bonneville Dam forebay elevations and discharge from the WSR. Dam forebay elevation changes over the first 3 weeks post-breach, when the sand bed was established in reach 2, are shown in Figure 17-A. The Bonneville pool was lowered from its normal elevation by >0.5 m during the dam breach, after which pool elevations were raised and then fluctuated by ~0.4 m. This amount of fluctuation would have a negligible effect on the observed deposition of the sand bed.

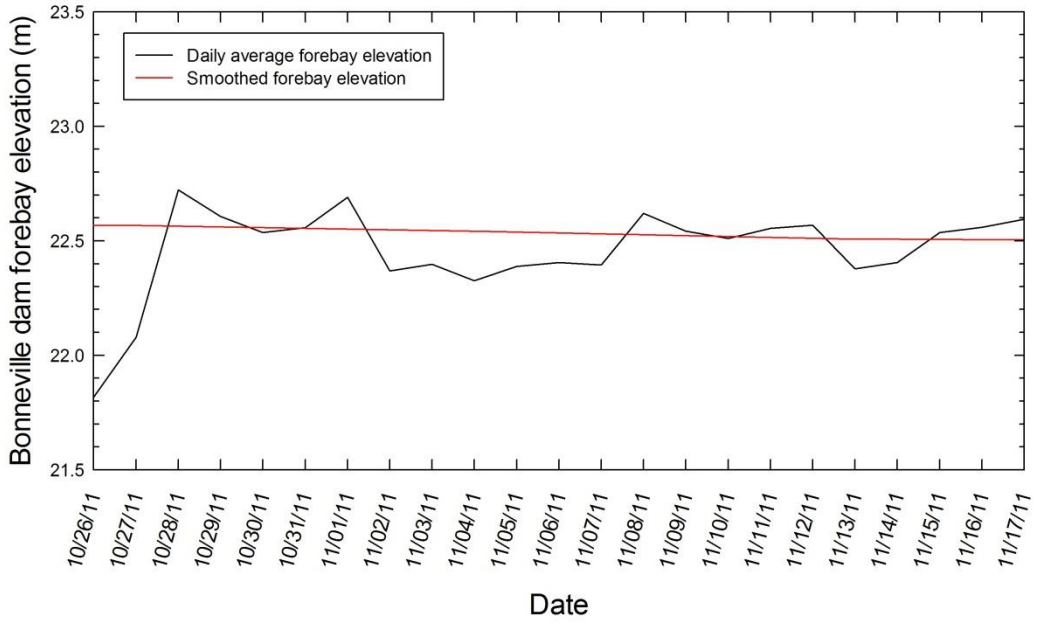

Figure 17-A: Bonneville pool elevations for first 3-weeks post-breach.

When forebay elevations are lower and the discharges are higher that there is a higher potential for geomorphic change in reach 2. Lower forebay elevations and higher discharges from late March to late May of 2012 may have promoted geomorphic change in reach 2 during this time (Figure 18-A).

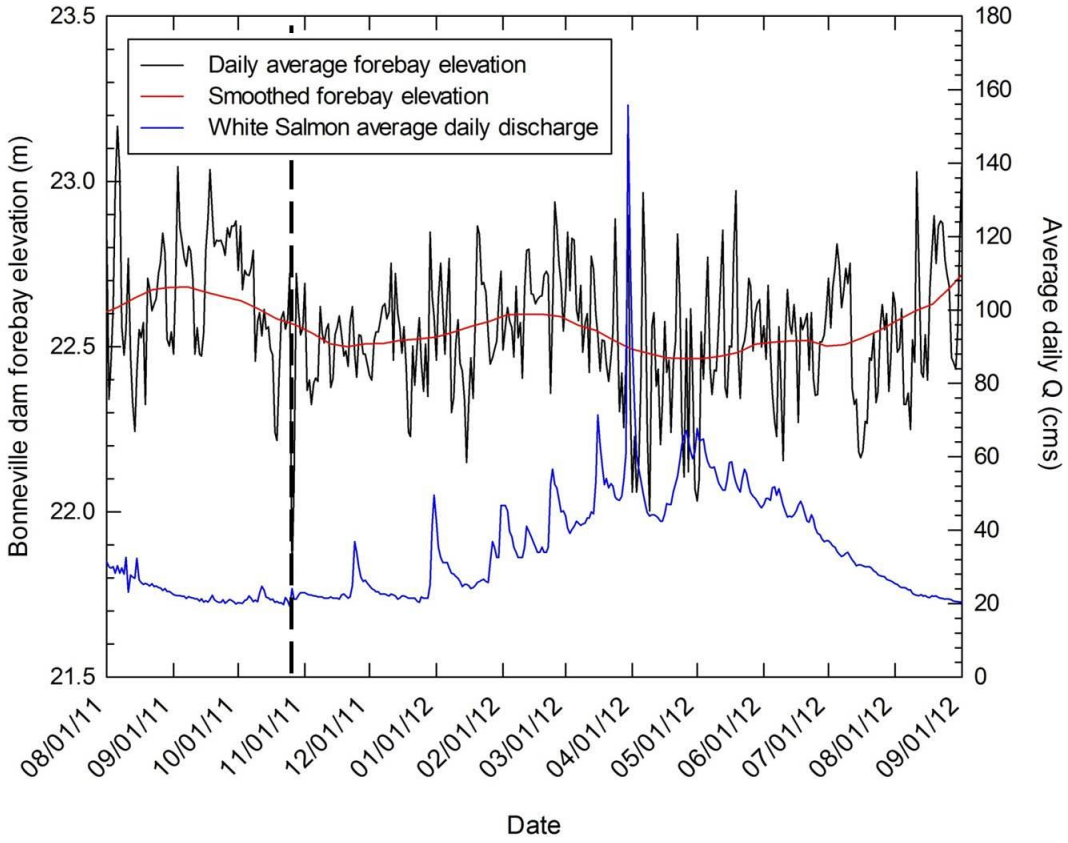

Figure 18-A: Bonneville Pool elevations (left y-axis) and average daily discharge (right y-axis) from Aug 1, 2011 to Sept 1, 2012. Time of dam breach shown by vertical dotted line.

APPENDIX G: PHOTOGRAPHS OF AGGRADED SAND BED

From dam site, river left, looking downstream (Jan 2012 photograph)

100 m downstream of dam, river left, looking upstream (Jan 2012 photograph)

100 m downstream of dam, river right, looking downstream at close-up view of aggraded sand bed terrace deposit (Aug 2, 2012 photograph)

125 m downstream of dam (cross section 1 location), river left, looking across river at right bank (Jan 2012 photograph

1,000 m downstream of dam, river left, looking upstream (Jan 2012 photograph)

1,900 m downstream, river left, looking downstream at powerhouse. Terrace visible on both left and right banks. (Jan 2012 photograph)

2,000 m downstream, river left, looking downstream from powerhouse. Terrace of aggraded sand bed seen on both left and right banks. (Dec 7, 2011 photograph from PacifiCorp Energy (2012))

3,100 m downstream, river left, looking upstream, standing on top of terrace. Terrace also visible in distance on right bank (Aug 2012 photograph)

3,100 m downstream, river left, angled downstream showing vertical face of terrace (Aug 2012 photograph)

3,700 m downstream, river left, facing downstream. Aggraded sand bed terrace visible on left bank (Jun 15, 2012 photograph)

3,700 m downstream, river left, close-up view of terrace shown in previous photograph (Jun 15, 2012 photograph)

3,700 m downstream, river right, looking at left bank. Sand bed terrace visible as horizontal, gray deposit above channel (Aug 14, 2012)

3,900 m downstream, river right, looking at left bank. Sand bed terrace visible as horizontal, gray deposit. (Aug 14, 2012 photograph)

3,900 m downstream, river right, up-close view of terrace face on right bank (Aug 14, 2012 photograph)

4,500 m downstream, river right, looking downstream towards right bank. Deposit of terrace is gray mass extending downstream from root wad (Aug 16, 2012 photograph)

5,000 m downstream, river right, facing downstream towards river mouth and Columbia. Terrace indistinguishable from deposited sand bar (Aug 16, 2012 photograph).

Photographs of low-angle cross-bedding within sand bed:

20 m downstream of dam, river right, looking towards bank

3600 m downstream of dam site, river right, looking towards bank